

Alma Mater Studiorum – Università di Bologna

Scuola di Ingegneria e Architettura

Dipartimento di Ingegneria dell' Energia Elettrica e  
dell' Informazione “G. Marconi”

Corso di Laurea Communication Networks, Systems and Services  
Ingegneria delle Telecomunicazioni

Tesi di Laurea in Propagation and Planning in Wireless Systems

**Performance Analysis of Ray-Tracing  
Assisted Beamforming Techniques for  
Future mm-wave Wireless Systems**

Candidato

Marco Zoli

Relatore

Ing. Franco Fuschini

Correlatori

Ing. Marina Barbiroli

Chiar.mo Prof. Gabriele Falciasecca

Anno Accademico 2014/2015

Sessione II



## ***Index:***

<i>Abstract</i>	<i>Pag.2</i>
<i>Introduction to Wireless Digital Communication</i>	<i>Pag.3</i>
<i>Multi-gigabit Wireless Systems</i>	
5G	<i>Pag.6</i>
mm-Waves	<i>Pag.7</i>
<i>Theoretical basics</i>	
Multi-antenna Systems	<i>Pag.10</i>
Beamforming Schemes	<i>Pag.14</i>
<i>Beam Searching and Tracking</i>	<i>Pag.24</i>
<i>Ray Tracing</i>	
General Description	<i>Pag.29</i>
Real Time Ray Tracing	<i>Pag.30</i>
<i>Ray Tracing based mm-wave Beamforming assessment</i>	
Study case	<i>Pag.32</i>
Multi-beams BF	<i>Pag.36</i>
Results	<i>Pag.40</i>
<i>Conclusions</i>	<i>Pag.44</i>
<i>Bibliography</i>	<i>Pag.45</i>

## ***Abstract***

*Il progetto di tesi riguarda principalmente la progettazione di moderni sistemi wireless, come 5G o WiGig, operanti a onde millimetriche, attraverso lo studio di una tecnica avanzata detta Beamforming, che, grazie all'utilizzo di antenne direttive e compatte, permette di superare limiti di link budget dovuti alle alte frequenze e introdurre inoltre diversità spaziale alla comunicazione. L'obiettivo principale del lavoro è stato quello di valutare, tramite simulazioni numeriche, le prestazioni di alcuni diversi schemi di Beamforming integrando come tool di supporto un programma di Ray Tracing capace di fornire le principali informazioni riguardo al canale radio. Con esso infatti è possibile sia effettuare un assessment generale del Beamforming stesso, ma anche formulare i presupposti per innovative soluzioni, chiamate RayTracing-assisted-Beamforming, decisamente promettenti per futuri sviluppi così come confermato dai risultati.*

# *Introduction to Wireless Digital Communications*

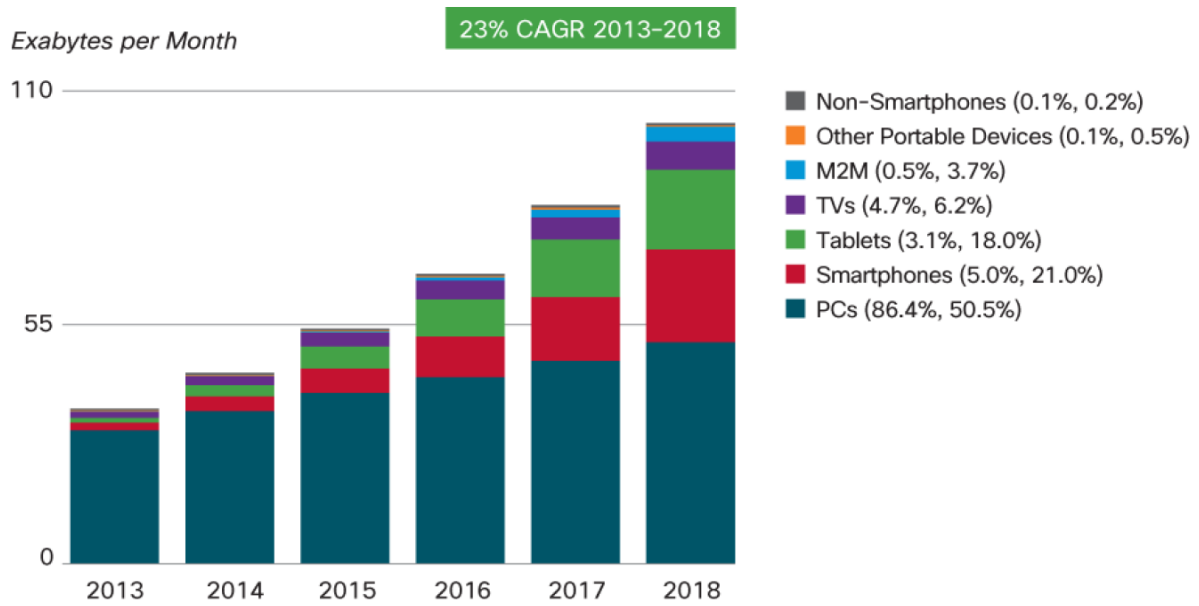
The history of telecommunications started long time ago in ancient time with optical and acoustic signals like fires and bells, but had a very crucial turning point when Guglielmo Marconi at the end of the 19<sup>th</sup> century, exploiting the long-range electromagnetic propagation, invented successfully the wireless telegraphy triggering the evolution of the modern broadcasting technologies like radio or television. The wireless communications, as well as Internet, have always had a worldwide big impact on trade, society and culture and nowadays they are still so: digital connectivity in recent years has become like a commodity, becoming soon one of the biggest dominant trend on the market, such that the world of Information and Communication Technologies (ICT), with smartphones, tablets, social networks, clouds and apps, has irreversibly penetrated into our common lives. From a general point of view what we are facing today is not only that a bigger number of people can access to Internet, the way of “consuming” information is radically changing: in [1] and in [2] Cisco talking about global internet traffic illustrates extraordinarily that ZettaByte Era is coming. This means a massively growing digital traffic demand all around the world, both in terms of volume and speed. The compound annual growth rate (CAGR) for the actual 2013-2018 period is around 60% for mobile data (Fig.1).

IP Traffic, 2013–2018							
	2013	2014	2015	2016	2017	2018	CAGR 2013–2018
<b>By Type (Petabytes [PB] per Month)</b>							
Fixed Internet	34,952	42,119	50,504	60,540	72,557	86,409	20%
Managed IP	14,736	17,774	20,898	23,738	26,361	29,305	15%
Mobile data	1,480	2,582	4,337	6,981	10,788	15,838	61%
<b>By Segment (PB per Month)</b>							
Consumer	40,905	50,375	61,439	74,361	89,689	107,958	21%
Business	10,263	12,100	14,300	16,899	20,016	23,595	18%
<b>By Geography (PB per Month)</b>							
Asia Pacific	17,950	22,119	26,869	32,383	39,086	47,273	21%
North America	16,607	20,293	24,599	29,377	34,552	40,545	20%
Western Europe	8,396	9,739	11,336	13,443	16,051	19,257	18%
Central and Eastern Europe	3,654	4,416	5,443	6,666	8,332	10,223	23%
Latin America	3,488	4,361	5,318	6,363	7,576	8,931	21%
Middle East and Africa	1,074	1,546	2,174	3,027	4,108	5,324	38%
<b>Total (PB per Month)</b>							
Total IP traffic	51,168	62,476	75,739	91,260	109,705	131,553	21%

Source: Cisco VNI, 2014

*Fig.1: Cisco Internet traffic prediction for 2013-2018.*

Moreover if we look in details at the differentiation among possible devices of the entire global traffic (Fig.2), the PCs percentage goes from 86,4% in 2013 to 50,5% in 2018, whereas smartphones from 5,0% in 2013 to 21,0% in 2018. An other evident aspect is represented by the Machine to Machine (M2M) devices growth that goes from 0,5% in 2013 to 3,7% in 2018.



Source: Cisco VNI, 2014

The percentages in parentheses next to the legend denote the device traffic shares for the years 2013 and 2018, respectively.

Fig.2: Cisco Internet traffic prediction for each category of digital device.

All these consideration are clear signs the mobile trend will be dominant in the following next years, making so wireless communications generally more and more important. In [3] Ericsson reports in fact other interesting results with an pleasant geographical partition (Fig.3):

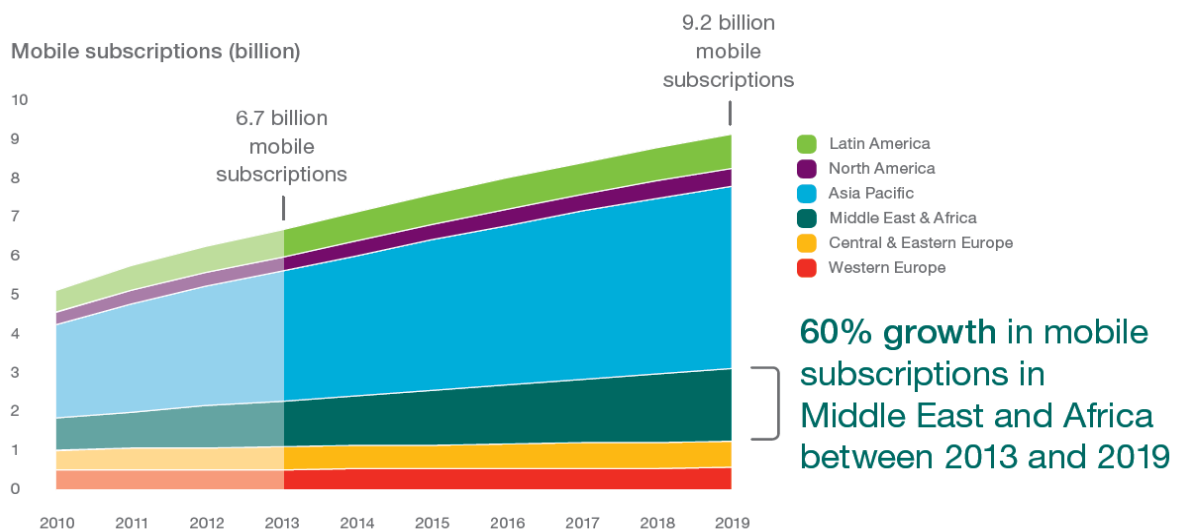
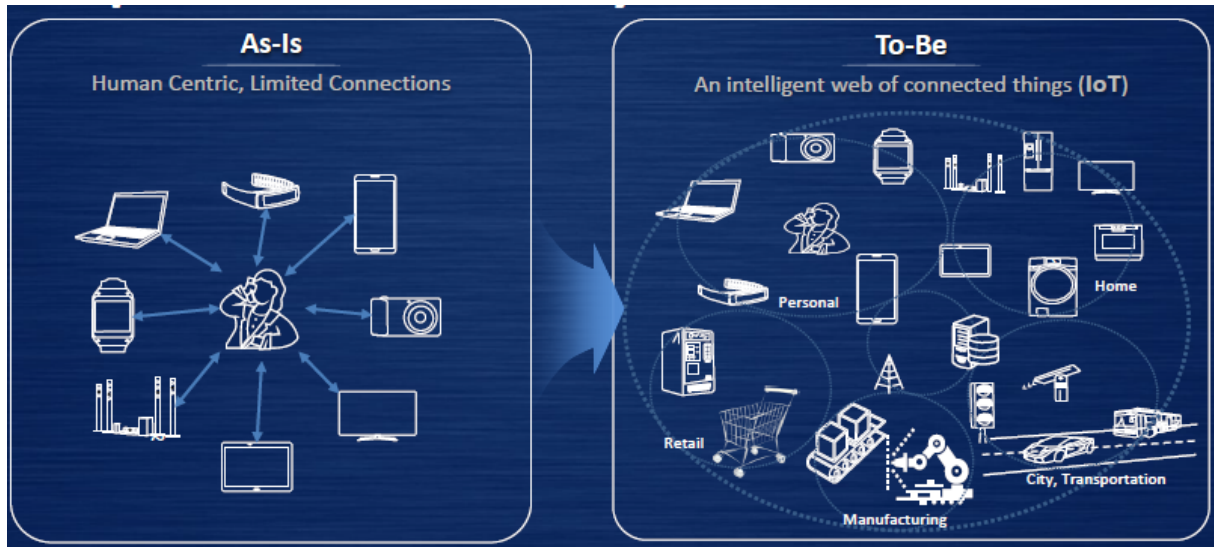


Fig.3: Ericsson mobile traffic prediction for each global macro-region.

Since Virtualization and Clouding technologies have had recently a huge effect on networks design, as discussed in [4], a new paradigm called Internet Of Things (IOT) - referred to the interconnection of uniquely identifiable embedded devices within the existing Internet infrastructure – seems to be really nearly upon us. Just think about Smart Cities, Smart Buildings, Smart Grids or even Intelligent Transportation Systems (ITS), a new revolutionary architecture for the future Internet network is becoming fundamental, (Fig.4). In conclusion, this new ICT ecosystem will involve for sure widespread investments and new solutions, both economically and technically, as defined, for instance, by European Horizon 2020 program. In particular for mobile communications, all of it will hopefully lead to a technological Renaissance where everything could be at best redefined for sustainability, efficiency and progress.



*Fig.4: Internet network transformation towards IoT.*

# Multi-gigabit Wireless Systems:

## 1) 5G

For the last several years a significant amount of research effort in the mobile communications has been investing in cellular and WiFi networks to provide higher data rates and better Quality of Service (QoS) at end users. For example 4G or LTE involves new excellent technologies like OFDMA, MIMO, CoMP, HetNet, CA and so on, with respect to the 3G, but it does not seem unfortunately to be a so advanced solution to support the future foreseen scenario. Thus the race to search for innovative systems like 5G has recently begun worldwide. No standard has been planned yet but a lot of new ideas are nowadays rising in R&D and Academia (Fig.5-6). Engineers, companies and industries has really started to think bigger, as outlined in [5 – 7]:

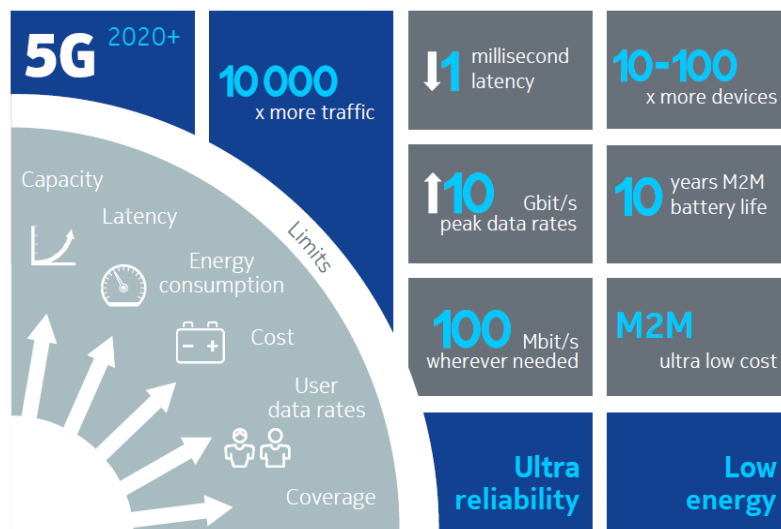


Fig.5: NOKIA about 5G.

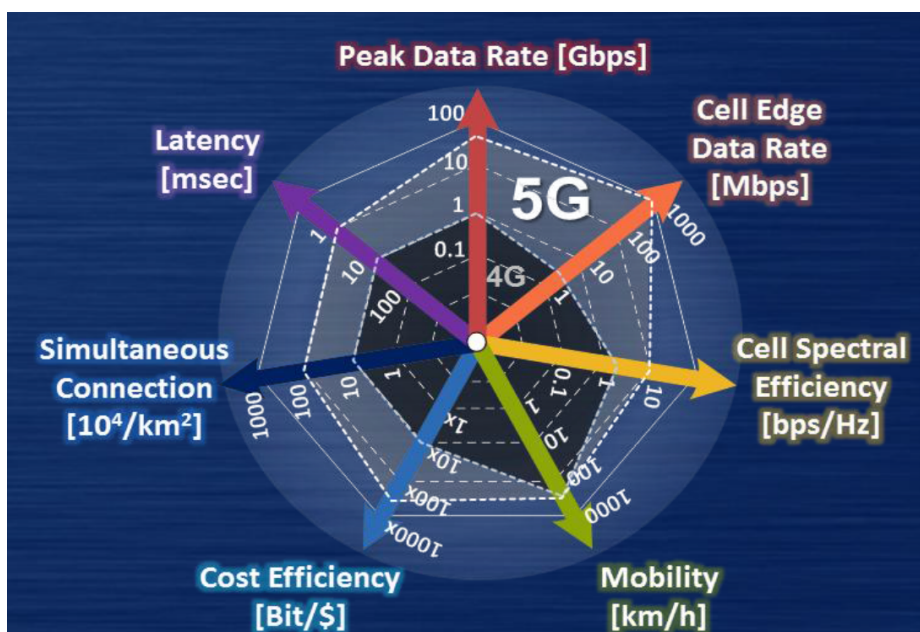


Fig.6: Samsung about 5G.



5G is still an open issue, but it could be much more than a new 3GPP standard: a symbiotic integration of novel and existing technologies, like 2G, 3G, 4G, WiFi, Personal Area Network (PAN), Body Area Network (BAN), Wireless LAN (WLAN), Wireless Sensor Network (WSN), M2M and even Device to Device (D2D) communications. Despite 5G and IoT concepts seem to lead to a chaotic and abstract framework, we know also that a smart and flexible spectrum management by ITU, -and CEPT in EU or FCC in USA-, can significantly strike the innovation. Just considering the 2G/3G bands re-farming done in Italy before the LTE licenses auction, hold at the end of 2011: each operator has gained new contiguous blocks for multi-carrier HSPA, -and so higher speed for 3G users-, and enough space for LTE channels, -and so new 4G users too-. Or just think about the 2.45GHz ISM band that is typically overpopulated by all 802.11 compliant technologies. Even if other concepts like Cognitive Radio or White Space Device could sound too extreme for practical implementations or profitable business, there is indeed today great interest in exploring new bands different from actual UHF frequencies -from 300 MHz to 3GHz-, in which large empty bandwidths are not so rare.

## 2) *Mm-waves*

As proved by recent research activities in academy [8][9], in industry [13][14] and in international standard organizations [10][11][12], the novel mm-wave wireless communications can be considered one of the best auspicious candidate for future systems, especially the bands of 60 GHz, that is available and unlicensed in most of the countries (Fig.7), and the 30 GHz too, as discussed in [15].

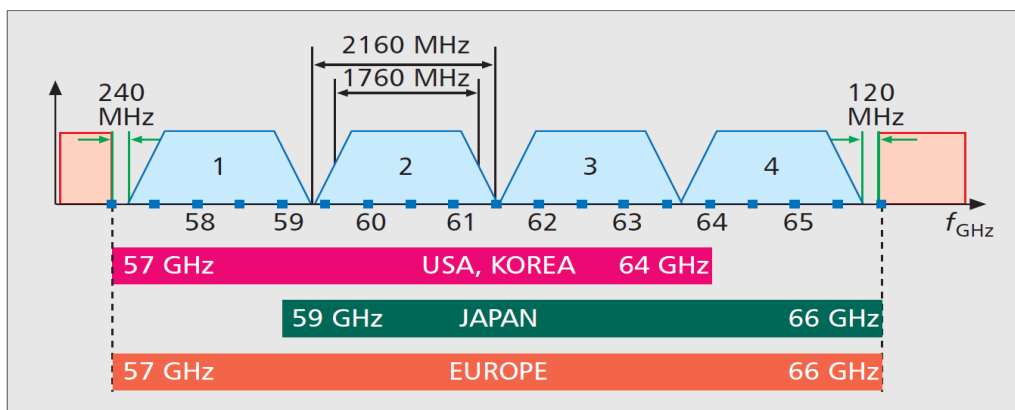


Fig.7: *four mm-wave channels in 57–66 GHz unlicensed band.*

The newest standard IEEE 802.11ad [12] and the related industry alliance named WiGig [13] -now in agreement with the IEEE 802.11 native WiFi alliance- show that the millimeter wave technology is really worth for multi-gigabit wireless communication, because compared to other traditional lower frequency systems, it holds several advantages including: huge free bandwidth up to 7 GHz, compact size of transceivers, due to small wavelength -roughly 5 mm- and, of course, the possibility to reach thousands of Mbps in the air, according to modern Modulation and Coding schemes. Furthermore, even though new RF modules, antennas, and electronics circuits must be redesign, in terms of spectrum utilization efficiency -that is bit / sec / Hz /squared meter-, a big convenience is clearly represented by this kind of unloaded bands -far away from usual 1 or 2 GHz ones- especially for very high speed multimedia applications like video streaming. However, there are several new hard challenges, mainly associated to the fact that mm-waves are more similar to light and so they act differently in the space in terms of electromagnetic propagation effects, like reflection, refraction, diffraction and scattering. For instance, high penetration loss and high path loss can really limit the range of coverage and make then the link budget more difficult to be balanced. As well as optics links, communications at 60 GHz can be very susceptible to line of sight (LOS)

blockage done by people or obstacles. To overcome all these problems, simply consequences of high RF carrier utilization, modern techniques as MIMO, Beamforming, directional multi-domain channel characterization and even Ray Tracing should be taken in consideration as very essential tools for the incoming future wireless systems. Taking as reference the Samsung study in [14], we can have a clear idea about what happens in practice: a comparison between a multi-antenna system at 30 GHz and 3 GHz single patch antenna (Fig.8). Moving from 3 GHz to 30 GHz we know that the path loss increases due to higher frequency, as trivially demonstrated by Friis's formula. If we choose for the RX a particular 8x8 array antenna with the same dimension of the patch, but able to provide highly directional beam, large gain and so good signal level strength, the path loss gap would be filled easily (Fig.9):

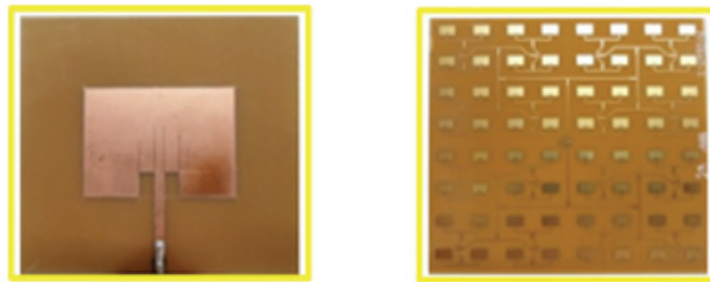


Fig.8: 3GHz and 30GHz antennas with same size.

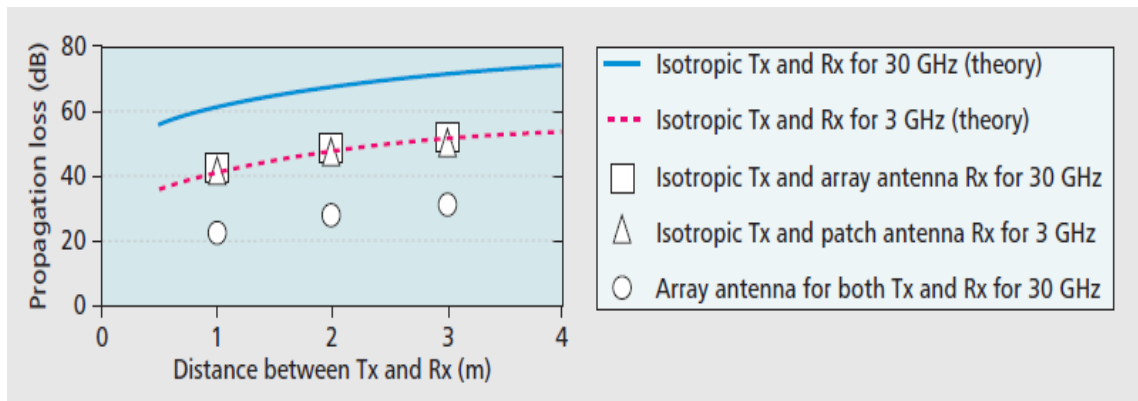
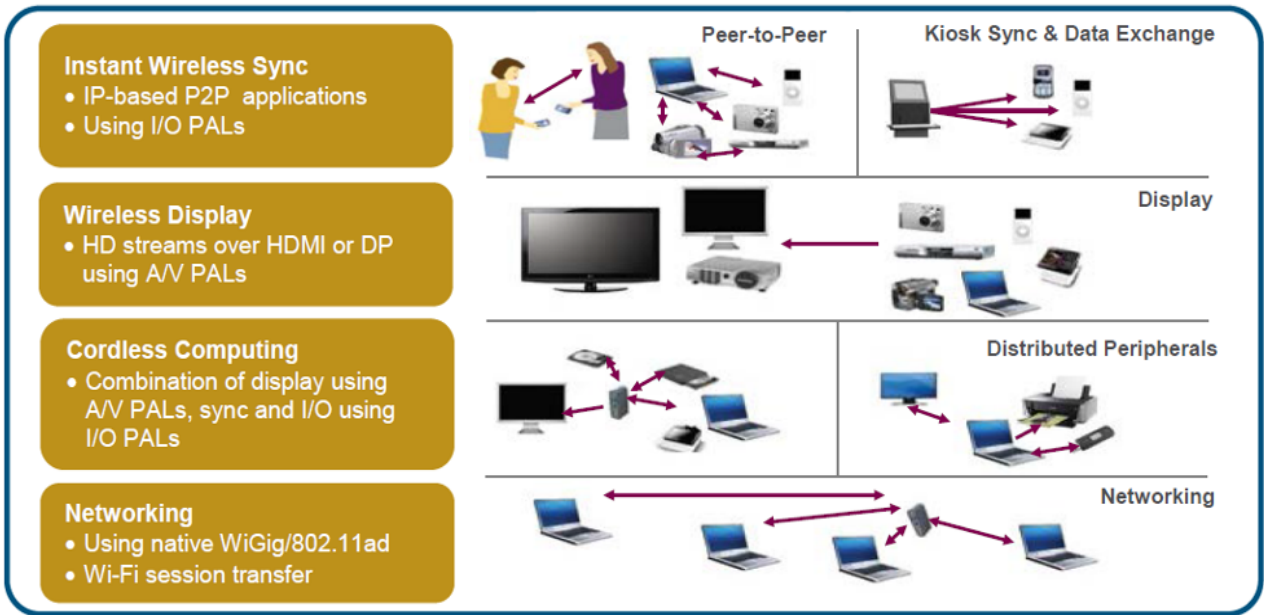


Fig.9: Path loss comparison.

Although several electronics difficulties occur at such high frequencies like high Phased Locked Loop (PLL) phase noise or non linear distortion, a lot of companies like Tensorcom [16], Wilocity [17], Qualcomm, Peraso, BeamNetworks, Silicon Image, and many others, are deeply involved in the development of 60 GHz chip-sets or devices, fully compliant to 802.11ad, thus suggesting that the mmWave emerging technology is getting ready, as confirmed by [18-21], and it will be soon present in the market probably with disruptive consequences.



*Fig.10: WiGig multimedia applications.*

# *Theoretical basics:*

## *1) Multi-antenna systems*

Multi-antenna systems consist of a set of antenna elements arranged together according to a predetermined geometry in order to increase the overall performance exploiting the spatial domain. For this reason, historically radar and sonar in military field have been the first main applications, but in the last decades multi-antenna systems have gained a lot of importance in civil wireless communications, because they allow to implement both spatial diversity to increase the SINR values and spatial multiplexing to achieve a considerable link capacity gain. In details these techniques can be enabled by Beamforming -that means, as we will discuss further on, shaping properly the antenna radiation patterns-, respectively setting more than one radiating beam towards the best directions that linked the TX/RX pair or allocating one radiating beam for each user RX, exploiting the space domain for multiplexing. The principal properties are the topology (linear, planar or volumetric), the single radiating element (isotropic, dipole, patch), the elements spacing distance (uniform or non uniform), the operating frequency (narrowband or wideband, with carrier or pulses) and, in the end, the different kind of electronic processing blocks. Despite multi-antenna systems imply for sure large cost and complexity, the capability to manage arbitrarily each antenna element in terms of feeding current represents a big advantage because the composite structure enable, in fact, a sort of spatial sampling, in the region where the antennas array is deployed, adding so further degrees of freedom to the traditional time signal processing. The fundamental principle of the antenna array analysis is the Pattern Multiplication. If possible mutual coupling effects occur, this rule, unfortunately, does not hold anymore and so the entire RF circuitry design must be optimally addressed by numerical e.m. simulators. As shown in [22], the radiated field of the multi-antenna system can be obtained by multiplying the single antenna element field -represented in the following section by a zero subscription- by a proper function that encloses all the spatial characteristics of the array itself, called Array Factor.

The electric field  $\mathbf{E}$ , under the far field approximation, is emitted by the array exactly with the same polarization of the single element field  $\mathbf{E}_0$  due to the scalar nature of array factor  $F$ :

$$\mathbf{E}(r, \theta, \phi) = \mathbf{E}_0(r, \theta, \phi) \cdot F(\theta, \phi). \quad [1]$$

Regarding the radiation intensity  $I_R$ , being proportional to the power of the field, in terms of watt over  $S_{rad}$ , must be related to the magnitude squared of the array factor  $F$ :

$$I_R(\theta, \phi) = I_{R0}(\theta, \phi) \cdot |F(\theta, \phi)|^2. \quad [2]$$

Pointing out the two angles  $\theta_{max}$  and  $\phi_{max}$  to which corresponds a maximum of radiation over the entire space of emission, we can express the normalized radiation intensity  $i_R$ , using the equivalent normalized array factor  $F_N$  and the single element normalized radiation intensity  $i_{R0}$ . This property is valid only in case of broadside without any radiating pattern alteration.

$$F_N(\theta, \phi) = \frac{|F(\theta_{max}, \phi_{max})|}{|F(\theta, \phi)|}. \quad [3]$$

$$i_R(\theta, \phi) = i_{R0}(\theta, \phi) \cdot F_N(\theta, \phi)^2. \quad [4]$$

Finally we get the total radiation function  $f$ , recalling the pattern multiplication rule. Cutting the 3D space with planes defined by  $\theta$  and  $\phi$  angles we can have the usual 2D radiation diagrams in the vertical and horizontal dimensions.

$$f(\theta, \phi) = \sqrt{i_R(\theta, \phi)} = f_0(\theta, \phi) \cdot F_N(\theta, \phi). \quad [5]$$

Moreover the overall gain  $G$  of array antenna, as usual, comes out from the maximal value of the directivity function  $D$ , with respect to a efficiency factor called  $\delta$ , that represent how much the antenna array is able to convert the feeding current into field waves, and viceversa, avoiding dissipation due to Joule effects:

$$d(\theta, \phi) = 4\pi \cdot \frac{I_R(\theta, \phi)}{\int_0^{2\pi} \int_0^\pi I_R(\theta, \phi) \sin\theta d\phi d\theta}. \quad [6]$$

$$G = d(\theta_{\max}, \phi_{\max}) \cdot \delta = D \cdot \delta. \quad [7]$$

Taking as reference the work in [23], we can show two significant concrete examples of multi-antenna where all the elements receive the same signal in terms of amplitude and phase and so the radiation pattern is expected to be broadside: the first one is a standard Uniform Linear Array (ULA) with  $N$  isotropic elements placed along  $z$  axis and equally separated by  $\lambda/2$  that has the following array factor  $F$ , for  $0 \leq \theta \leq \pi$ , (Fig.11):

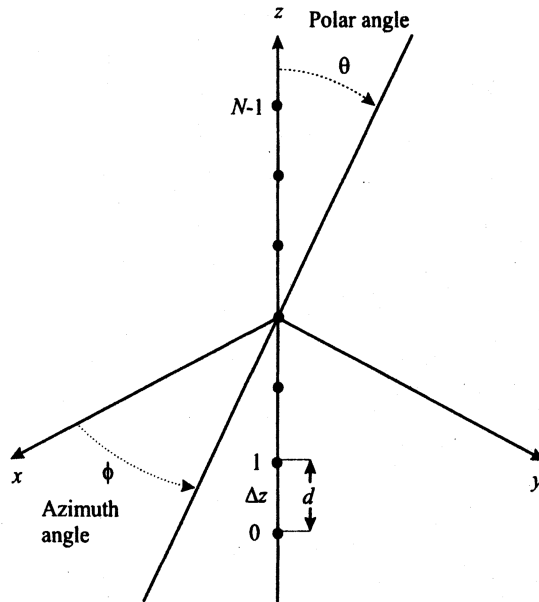


Fig.11: standard ULA configuration.

$$F(\theta) = \frac{1}{N} \cdot \frac{\sin(\pi \cos(\theta)N/2)}{\sin(\pi \cos(\theta)/2)}. \quad [8]$$

It is easy to see that  $F$  depends only on  $\theta$  because the array is deployed only along one direction. This means we can shape the radiation pattern only in the vertical plane, the one that contains the

antennas array, (Fig.12). All the characteristics of the  $\phi=0^\circ$  cut plane diagram are summarized in the following table. It is worth to note the relative contribution of the single element pattern that multi-antenna array is made of, is not taken into account for sake of generality.

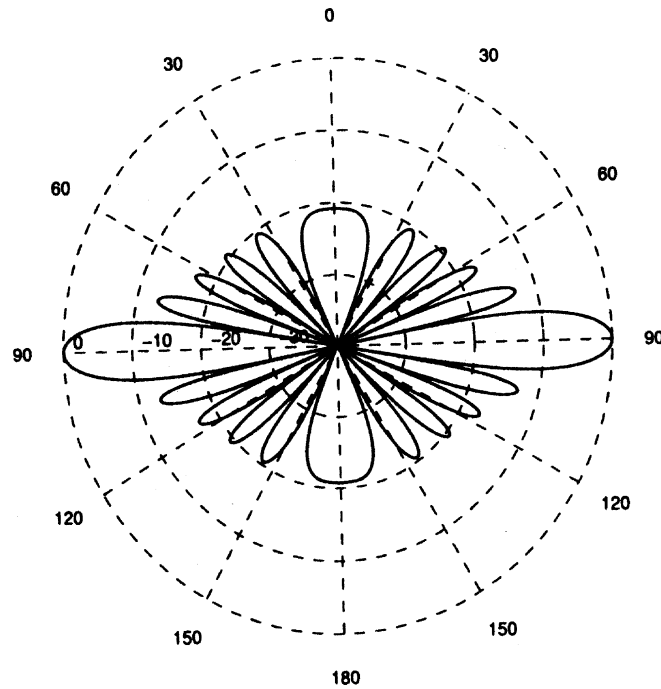


Fig.12: Polar plot of ULA array factor,  $\phi=0^\circ$ .

3dB HalfPowerBeamWidth	$\approx 102.1 / N$ degrees
Null to null distance	$\approx 4 / N$ radians
Directivity	$\approx N$

The second one is a standard Uniform Rectangular Array (URA) with  $N \times M$  isotropic elements placed along  $x$  and  $y$  axis and equally separated by  $\lambda/2$ , that has the following array factor  $F$ , for  $0 \leq \theta \leq \pi$  and  $0 \leq \phi \leq 2\pi$ , (Fig.13):

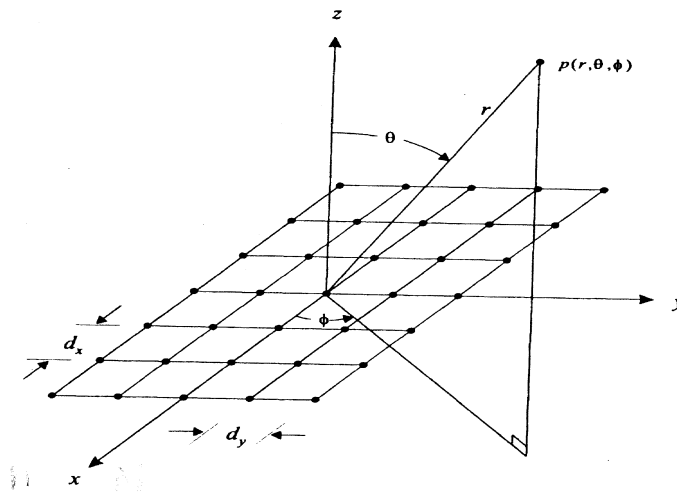


Fig.13: standard URA configuration.

$$F(\theta, \phi) = \frac{1}{N} \cdot \frac{\sin(\pi \sin(\theta) \cos(\phi) N/2)}{\sin(\pi \sin(\theta) \cos(\phi)/2)} \cdot \frac{1}{M} \cdot \frac{\sin(\pi \sin(\theta) \sin(\phi) M/2)}{\sin(\pi \sin(\theta) \sin(\phi)/2)}. \quad [9]$$

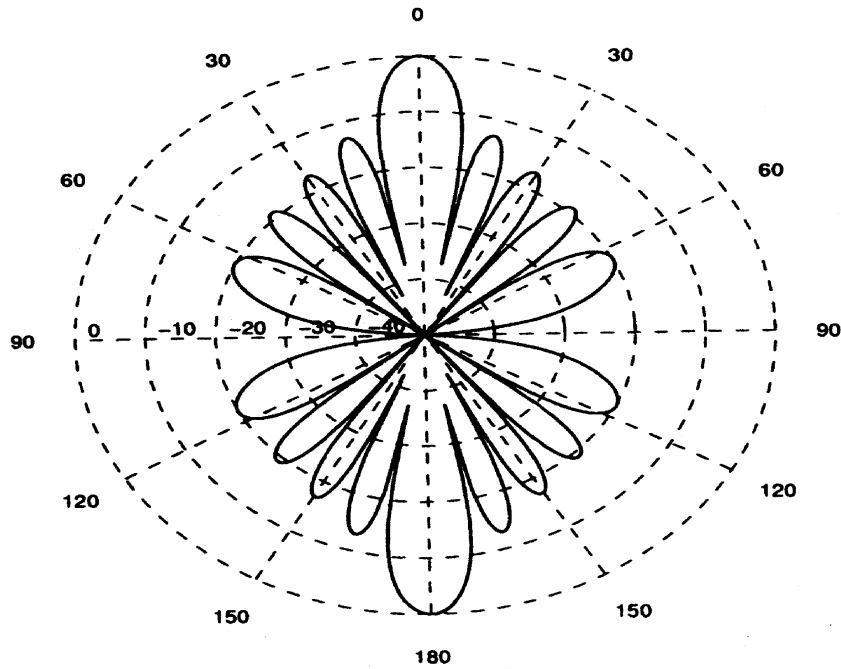


Fig.14: Polar plot of URA array factor,  $\phi=0^\circ$ .

Since this planar array is a cross-mix of two independent linear array along x and y directions, all the characteristics for the  $\phi=0^\circ$  cut plane radiation diagrams are the same of the ULA case, both in x and y respectively, but the D that is now proportional to  $N \cdot M$ , (Fig.14). As discussed in the previous chapters, this kind of antennas are very suitable for next mobile wireless communications, like 5G or WiGig: the small wavelength of mmWave facilitate the use of massive MIMO antenna in compact form factor (Fig.15), typically few cm squared, as in [16]:

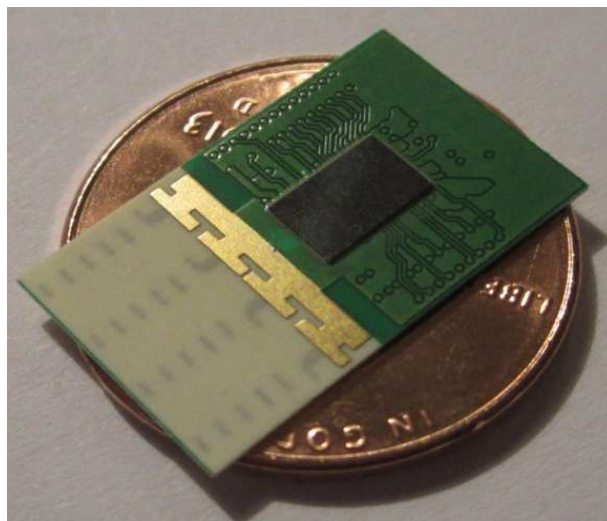


Fig.15: Tensorcom 60GHz multi-antenna.

Advanced technique like Spatial Diversity -that aims at improving the quality of communication in terms of SNR and BER with combining techniques like MRC- or Spatial Multiplexing -that aims at increasing the capacity of the link data rate with processing scheme like Space Time coding- can

really make the mmWave links reliable and fast. The price to pay is the fundamental knowledge of the Channel State Information (CSI), that is strictly compliant to the secret nature of the radio channel in terms of multipath richness and stationarity.

## 2) Beamforming Schemes

Beamforming (BF) -that means semantically the capability of piloting multi-antenna elements in order to shape arbitrarily the overall radiation pattern beams- aims, differently from previous cases, at boosting the strongest multipath contribution to achieve higher SINR. It does not benefit by multipath or uncorrelation, in principle, but it turns the space domain into a extra resource in the communication. It needs therefore the right positions coordinates of the TX/RX couple because the radiation pattern must be optimally modified or to focus at TX side the total available power in the best direction or to select at RX side the right solid angle of incoming fields. Generally, as in [23], the study of array antennas for Beamforming can be carried out starting from the following case:

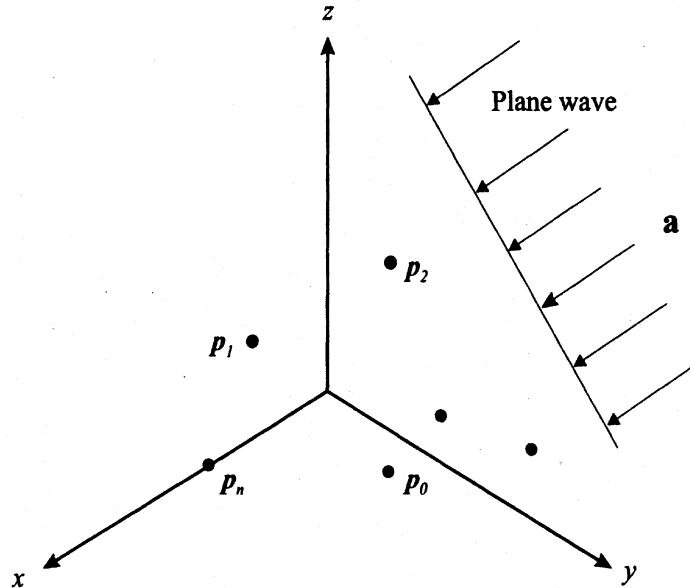


Fig.16: plane waves on ideal antenna array.

Considering incoming single frequency plane waves propagating along direction  $\mathbf{a}$ , in a locally homogeneous medium, around an ideal abstract receiver, that is composed by  $N$  elements located at  $[\mathbf{p}_0, \dots, \mathbf{p}_{N-1}]$  positions, (Fig.16), we can express the wave-number  $\mathbf{k}$  as:

$$\mathbf{k} = \frac{2\pi}{\lambda} \mathbf{a}. \quad [10]$$

Then, the particular vector that includes all the spatial characteristics of the array, given its topology, is called array manifold vector  $\mathbf{v}$ :

$$\mathbf{v}(\mathbf{k}) = \left[ \exp(-j\mathbf{k}^T \mathbf{p}_0), \exp(-j\mathbf{k}^T \mathbf{p}_1) \dots, \exp(-j\mathbf{k}^T \mathbf{p}_{N-1}) \right]^T. \quad [11]$$

BF can be theoretically performed by imposing, to each branch of the antenna array, a specific complex weight  $\mathbf{w}_i$  able to properly modify the signal both in amplitude both in phase (Fig.17); (the 'c' states for complex conjugation):



$$\mathbf{w}^H = [\mathbf{w}_0^c, \mathbf{w}_1^c \cdots, \mathbf{w}_{N-1}^c]. \quad [12]$$

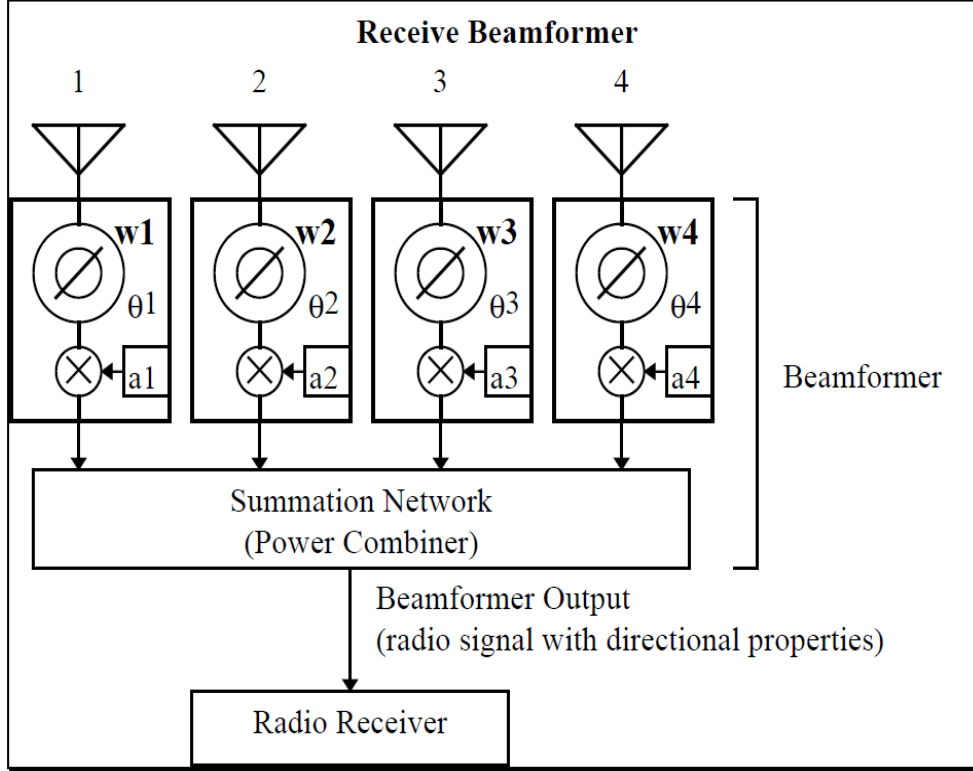


Fig.17: four elements beamforming receiver scheme.

Finally, the array factor  $F$  can be expressed by this scalar product:

$$F(\omega, \mathbf{k}) = \mathbf{w}^H \cdot \mathbf{v}(\mathbf{k}). \quad [13]$$

Recalling the ULA and URA examples in equations 8 and 9, respectively, the general-purpose array factors, now conditioned by weightings, can be expressed by:

$$F(\theta) = \exp(-j \frac{N-1}{2} \pi \cos \theta) \sum_{n=0}^{N-1} w_n^c \cdot \exp(j n \pi \cos \theta). \quad [14]$$

$$\text{set: } u_x = \sin \theta \cos \phi ; \quad u_y = \sin \theta \sin \phi ;$$

$$F(\theta, \phi) = \exp(-j \frac{N-1}{2} \pi u_x - j \frac{M-1}{2} \pi u_y) \sum_{n=0}^{N-1} \sum_{m=0}^{M-1} w_{nm}^c \cdot \exp(j n \pi u_x + j m \pi u_y). \quad [15]$$

Now we can see that the Array Factors are not written in closed formulas as in equations 8 and 9 because they strongly depend on the weights series. Of course the complete radiating pattern can be achieved only adding the information about the single radiating antenna element using the pattern multiplication rule. All these considerations, that come directly from classical array theory as in books [24-30], hold only in case of narrowband signal and without antenna mutual coupling effects. The basic concept, behind any actual combining or filtering scheme, like BF, is the “delay and sum” scheme called also conventional beamformer. Correctly “co-phasing”, with the use of generic elaboration blocks  $h_n(\tau)$ , the different replica of the incoming collected signal  $f(t, \mathbf{p}_n)$ , all the

contributions can be summed constructively increasing as result the SNR of the output  $y(t)$ .

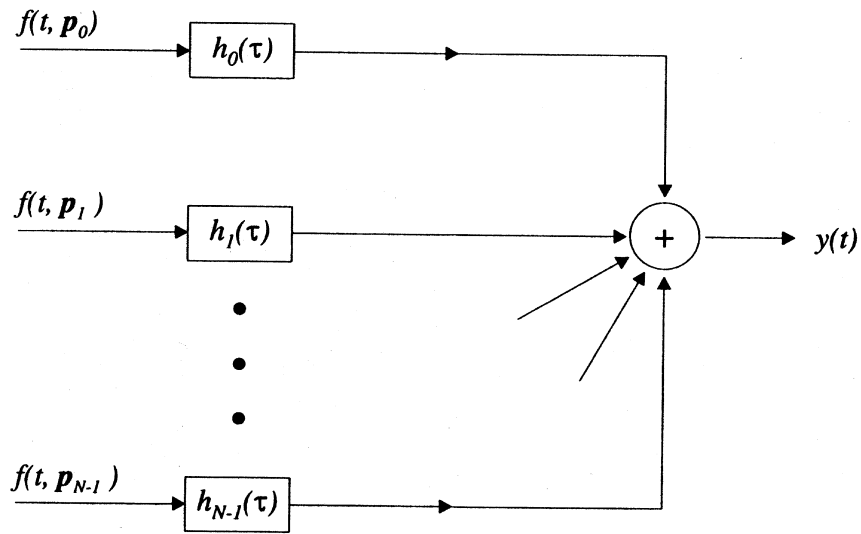


Fig.18: Delay and Sum scheme.

This idea can be practically developed in several ways:

**1 - Analog BF** is typically performed in the RF analog front end using T/R modules composed by VGA amplifiers and phase shifters, that can be even controlled digitally, (Fig.19-20):

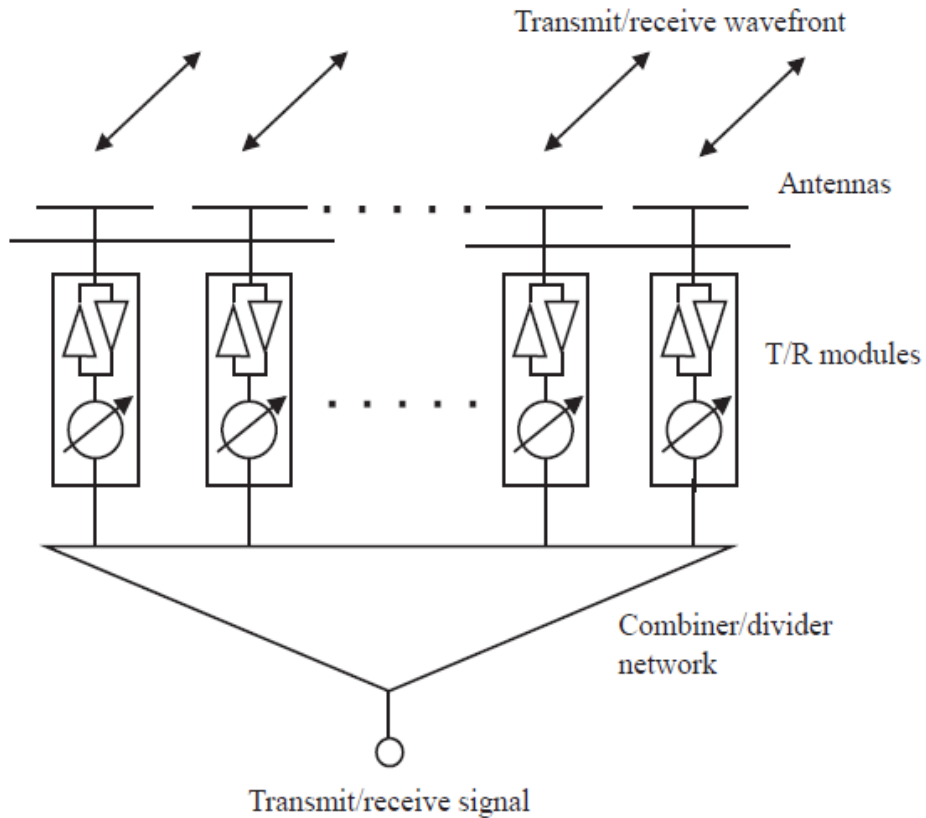


Fig.19: analog beamforming transceiver scheme.

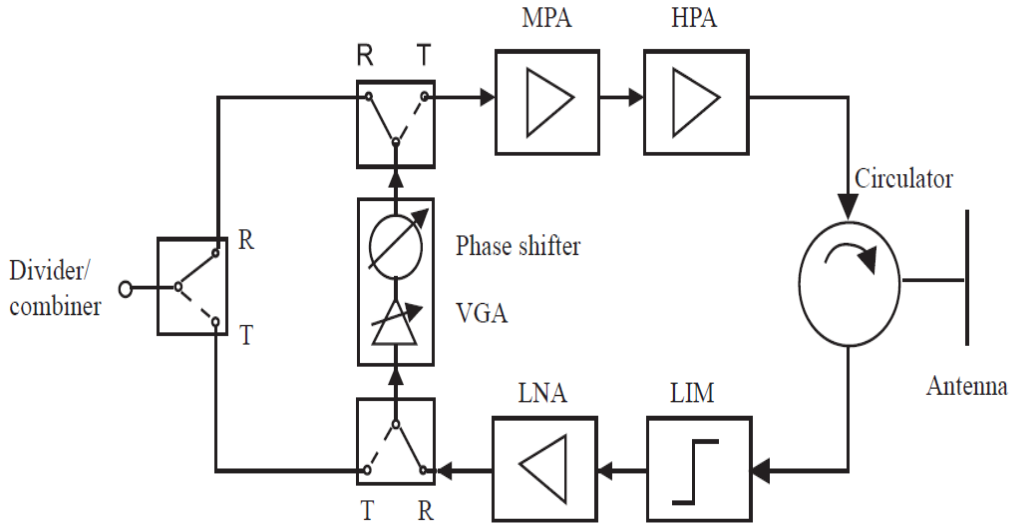


Fig.20: T/R modules block diagram.

This solution is capable to steer the array main response axis (MRA) towards any direction. This is also known as electronic steering of the radiation beam, differently from mechanical steering used in the past. For instance, calling  $\mathbf{k}'$  the target wave-number in k-space which BF combining weights shall be compliant to, taking as reference the ULA case with uniform amplitude weighting and recalling equation 13, we get:

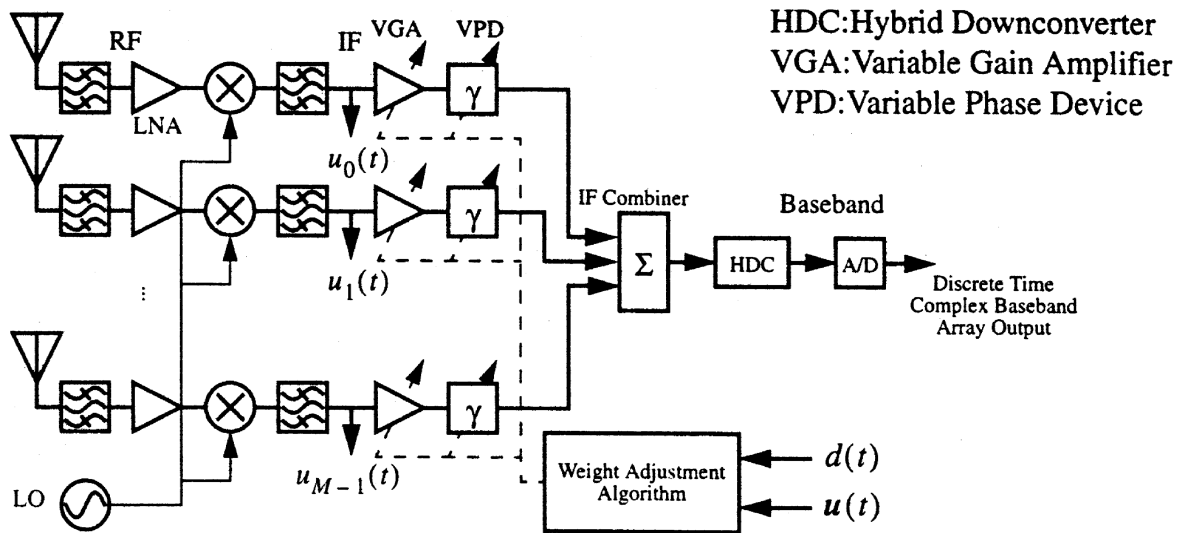
$$\mathbf{w} = \frac{1}{N} \mathbf{v}(\mathbf{k}') \quad [16]$$

$$F(\mathbf{k}) = \frac{1}{N} \cdot \mathbf{v}^H(\mathbf{k}') \cdot \mathbf{v}(\mathbf{k}). \quad [17]$$

In terms of vertical angle  $\theta$ , the right steering direction, called  $\theta'$ , for ULA antenna is a simple angle shift in the array factor formula:

$$F(\theta) = \frac{1}{N} \cdot \frac{\sin(\pi[\cos(\theta) - \cos(\theta')]N/2)}{\sin(\pi[\cos(\theta) - \cos(\theta')]/2)}. \quad [18]$$

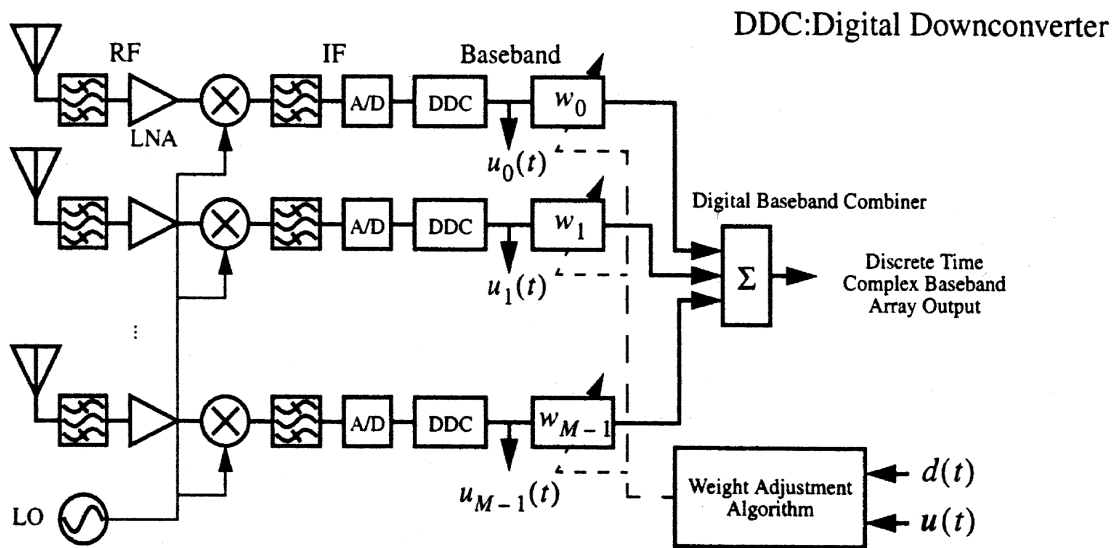
Of course the radiation pattern changes sinuously according to the applied weights but the main lobe width can become larger and the directivity could decrease too. This kind of trade off is valid for every array and it represents a bound for adaptability. The limit case is represented by  $\theta' = 180^\circ$  where the array pattern becomes end-fire and then the main lobe is aligned to the array structure axis. In conclusion we can have look at Fig.21 where a complete analog BF receiver is sketched:



(a) Analog IF weighting and combining

Fig.21: a complete analog BF receiver scheme.

**2 - Digital BF**, (Fig.22), is much more flexible than analog BF but it needs for each antenna element a complete RF chain. In this solution the weights are really complex number that are applied directly in base-band domain into signals samples sequences, like FIR/IIR filters or other combining techniques. However the power consumption of the ADC is directly proportional to sampling frequency, which may be in the order of GHz for 60 GHz transceiver system, and so it could become a serious problem for mm-Wave applications.



(b) Digital complex baseband weighting and combining

Fig.22: digital BF receiver.

**3 - Hybrid BF** solutions are the right choice in order to cope with the trade off between complexity and flexibility. The first example (Fig.23), regards a sub-arrays Beamforming where some elements of the array are grouped together and processed uniquely to reduce the required number of parallel RF chains.

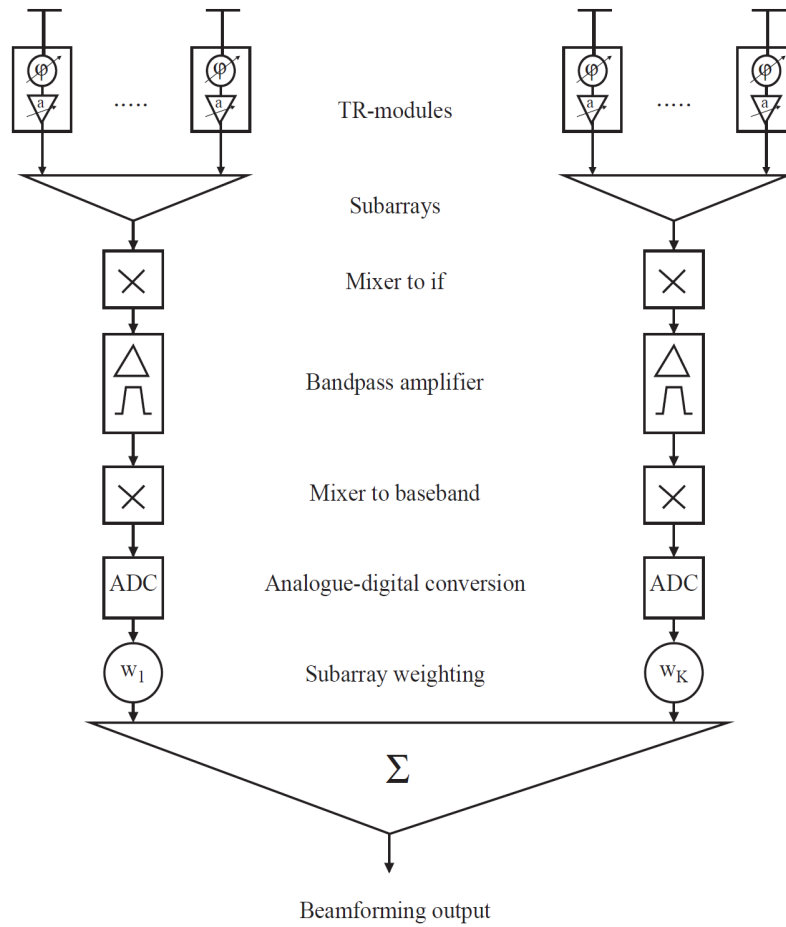


Fig.23: two subarrays hybrid beamformer scheme.

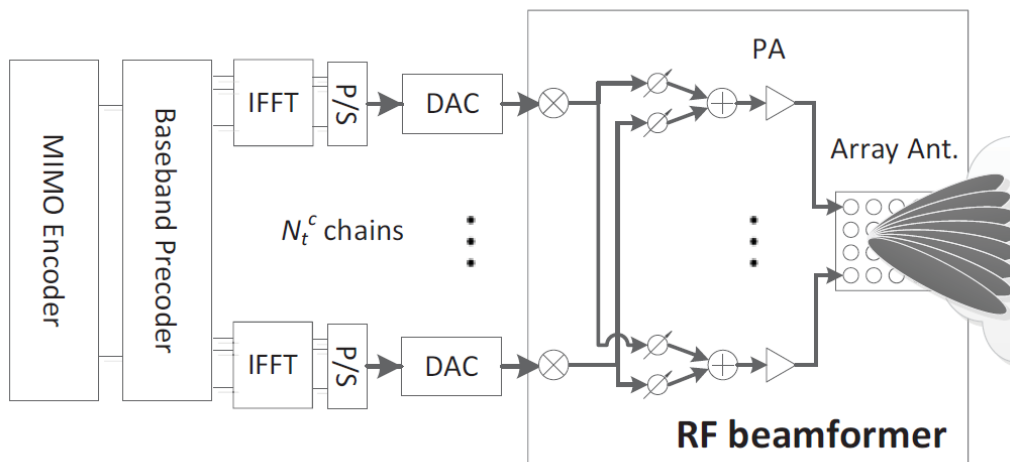


Fig.24: hybrid solution TX with OFDM.

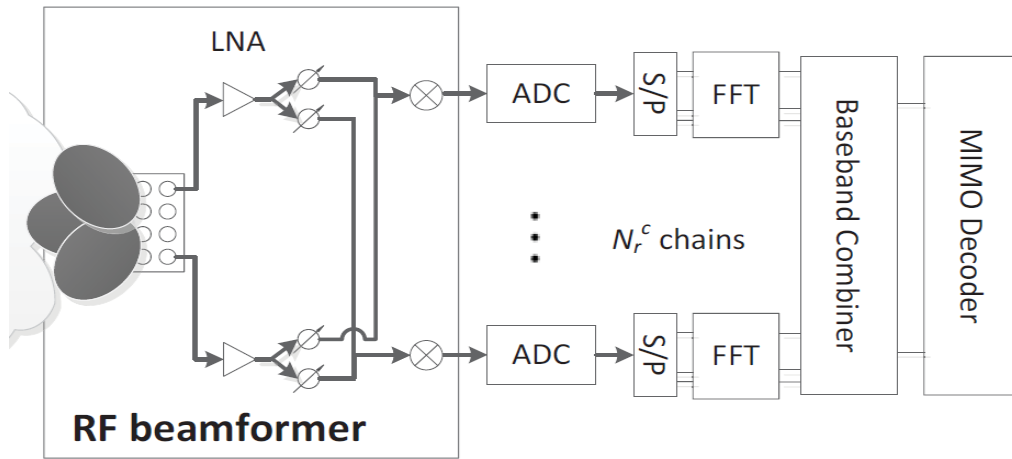


Fig.25: hybrid solution RX with OFDM.

The second example (Fig.24-25), taking as reference [14], is a modern complete TX-RX blocks diagram where the BF is included into the well-known OFDM scheme. In conclusion in case of wideband signals everything must be revised because all the antenna properties may vary significantly over frequency. Beamformer based on FFT algorithm and advanced DSP techniques are the right way to follow in this case, (Fig. 26):

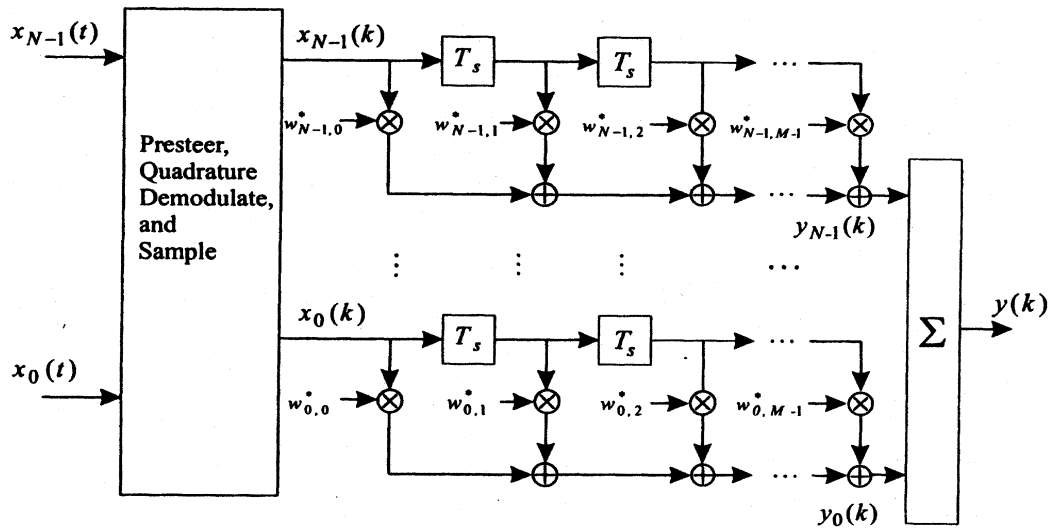


Fig.26: example of wideband beamformer block diagram.

Once the BF basics have been outlined, the picture about BF would not be complete without the design part that is named antenna array synthesis process: given a desirable radiating pattern, how to choose at best the weights coefficients? For equally spaced array, the array factor can be considered exactly the form of DFT of the weights and so the techniques from equivalent temporal filters can be used directly. Recalling, for simplicity, the ULA case and taking again as reference the discussion in [23]:

calling:  $\psi = \pi \cos \theta$ ; ( $-\pi \leq \psi \leq +\pi$ )

$$F(\psi) = \exp(-j \frac{N-1}{2} \psi) \sum_{n=0}^{N-1} [w_n \cdot \exp(-j n \psi)]^c. \quad [19]$$

calling:  $z = \exp(j \psi)$ ;

$$F(z) = z^{-\frac{N-1}{2}} \cdot \sum_{n=0}^{N-1} [w_n \cdot z^{-n}]^c. \quad [20]$$

It easy to see that the equation 20 is similar to Z transform that is a typical math tool of DSP area. Then getting N sampling points of the wanted array factor, we reach immediately the DFT expression in equation 21:

$$\text{calling: } z_k = \exp(j \frac{2\pi}{N} \cdot (k - \frac{N-1}{2})); \quad (k=0,1,\dots,N-1)$$

$$\text{calling: } b_n = w_n \cdot \exp(j n \pi \cdot \frac{N-1}{N}); \quad (n=0,1,\dots,N-1)$$

$$F_k = \sum_{n=0}^{N-1} b_n \cdot \exp(-j k n \frac{2\pi}{N}). \quad [21]$$

Everything can be seen also in algebraic form using, as usual, a matrix  $\mathbf{M}$ :

$$\mathbf{F} = \mathbf{M} \cdot \mathbf{b}. \quad [22]$$

$$\mathbf{b} = \frac{1}{N} \mathbf{M}^{-1} \cdot \mathbf{F}. \quad [23]$$

$$w_n = b_n \cdot \exp(-j n \pi \cdot \frac{N-1}{N}). \quad [24]$$

Summing up, if we know  $\mathbf{F}$  in N samples points, arbitrarily chosen, we can also find  $\mathbf{b}$  and so  $\mathbf{w}$  using the IDFT Weight Vector Determination algorithm just pointed out here in equations 23 and 24. This is only an example for the 1D case, but all of it is also valid for 2D or 3D cases with the corresponding DFT formulas. Moreover, as well as in FIR/IIRs the discrete coefficients can be modified with windows processing in order to shape the frequency response of filters, we may make use of the same windowing functions on BF weights vector in order to control, in this case, the overall radiation pattern of the array. Choosing different amplitudes and phases among Hann, Hamming, Blackmann-Harris, Kaiser, Cosine-m, DPSS, Dolph-Chebyshev, Taylor, Villeneuve windows, we can totally manage the side-lobes levels, the HPBW and null-to-null distance properties.

Considering now a real scenario where the total e.m. field includes interference, noise and useful signals around the receiver space, we can soon realize that the broad BF objective is nothing else than an optimization problem of the SINR. This mean practically synthesizing a pattern with maxima beams towards useful signals and null beams towards interference sources. Least Squares Error Pattern Synthesis, for example, is a valid algorithm for this purpose, as in [23]. Furthermore,

knowing the properties of feedback loops and estimation-decision theory, if we compute the complex weights and update them in real time, -depending on the hypothesis made about signals, noise and interference of course-, we can build an adaptive BF, as well as it happens for DSP processing or demodulation/decoding blocks in modern wireless terminals, (Fig.27). In literature -see always [23]- several schemes have been proposed: MVDR, MPDR, LCMV, LCMP, MMSE.

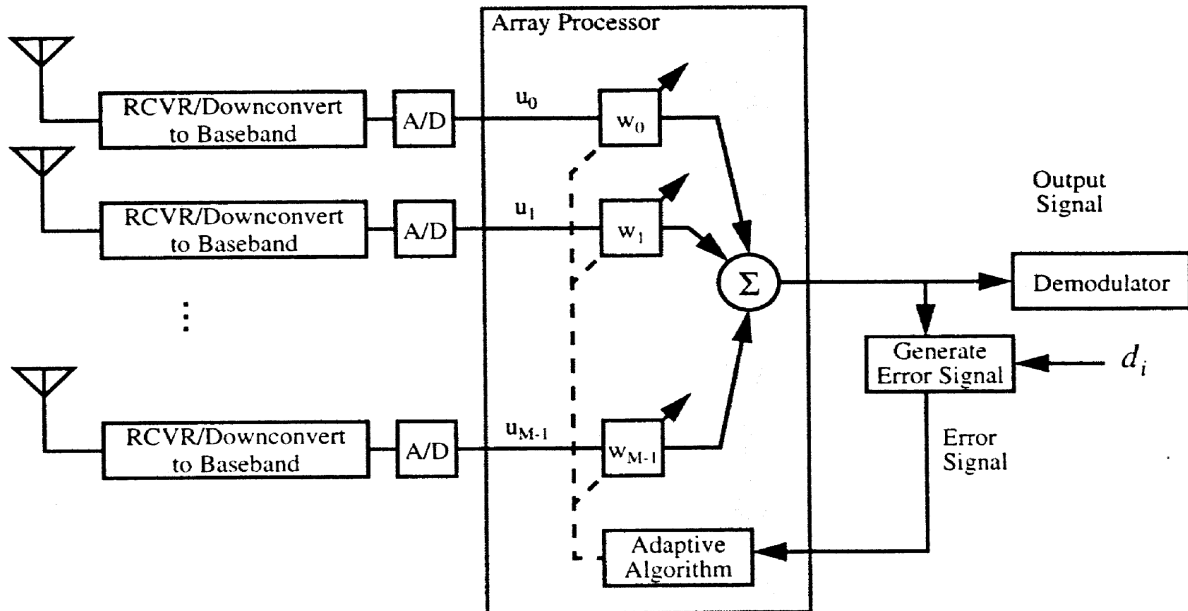


Fig. 27: example of adaptive BF scheme.

In order to complete the discussion about the revolutionary capabilities of Beamforming, we shall take into account an example of a Base Station in multi-users cell, (Fig.28):

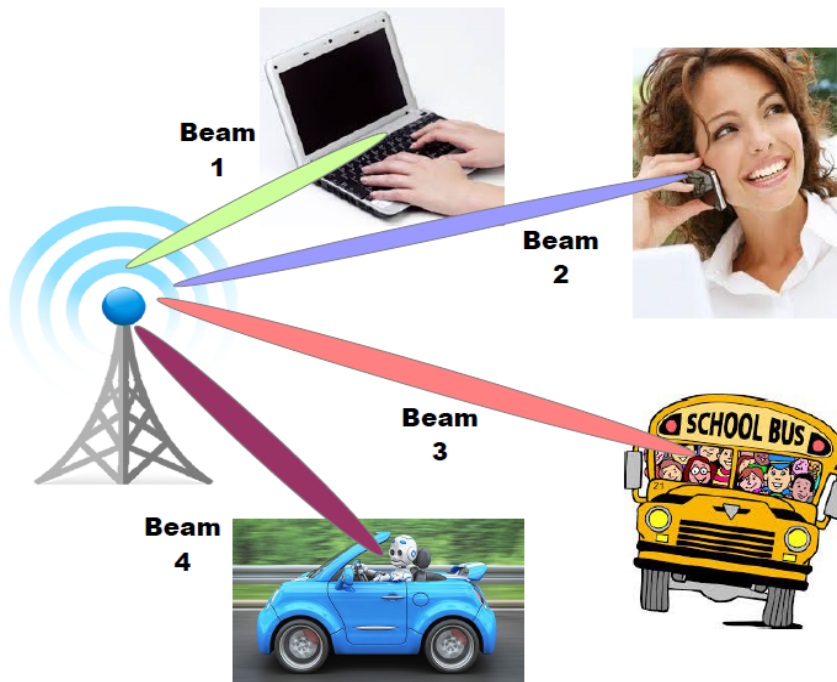


Fig.28: SDMA example with four beams.



Typically a cell is subdivided in three sectors and different users are served using a dynamic allocation of radio resources, like channels, slots or codes. Spatial Division Multiple Access (SDMA), instead, on the basis of BF technique, uses the angular/space domain to physically separate the different data streams into different spatial beams through the use of smart antennas. The main clear advantages are less wasted energy, greater gain, less interference and even unitary frequency reuse. Unfortunately, the Base Station must know exactly where the users are and even track them during all the down/up links communications. BF smart antennas, furthermore, have other intrinsic limitations: the number of beams hardly can be comparable with the number of common users served in a cell and also the spatial resolution is limited. This means that a group of users, that are too close each other, can not be served at the same time. Here below the Fig.29 shows a theoretical multi-users BF for SDMA applications diagram -in this case only two user A and B, for sake of simplicity, has been considered-. The steering BF weights are applied to each input signals and then linearly summed in order to make the antenna array to generate two divided beam patterns superimposed.

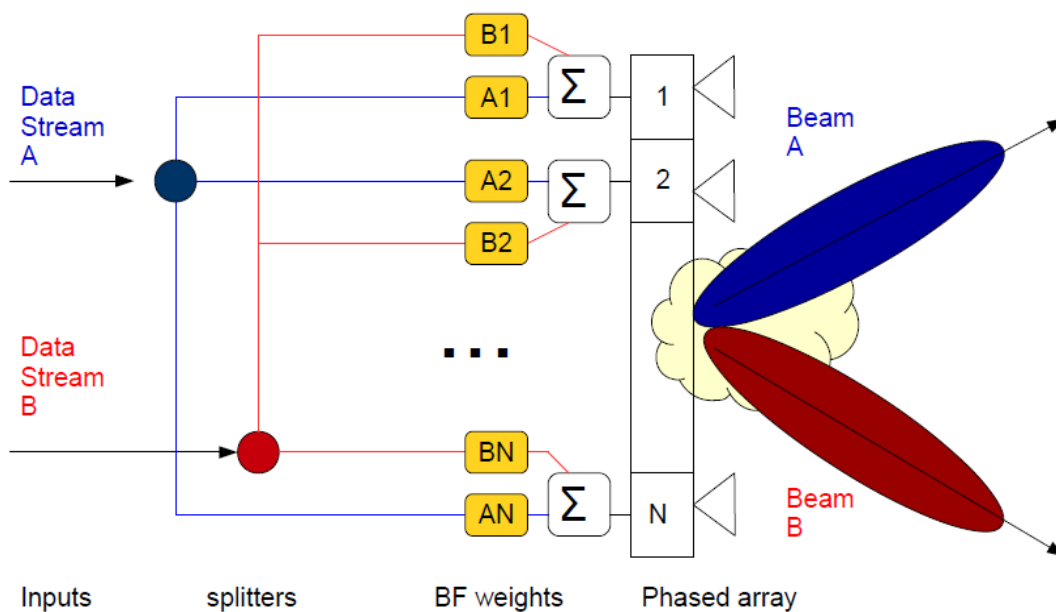


Fig.29: dual-beams Beamforming scheme for SDMA.

## *Beam Searching and Tracking*

One big problem for BF implementation still remains crucial: how to evaluate at receiver side, the right angles, called AoA or DOA, of the incoming signals? how to obtain the best information about the transmitter position? Well-known algorithms like MVDR, MUSIC, ESPRIT, with all possible variants, can be optimally implemented but they require anyway an high level of complexity, in terms of digital estimation and elaboration, as discussed in [23]. Other possibilities can be represented by GPS or other localization systems or even terminals databases, but they are far away from compatibility and easiness nowadays. Ray Tracing or Ray Launching, in the end can results a good candidate as strong enabler for BF and MIMO technology, as explained in the following chapters. Anyway this big issue, often named as Beam searching or Beam tracking, is far from being solved because it involves both BF architectures capabilities at physical layers, as previously described, and also general protocols at Data Link or MAC layers too. The TX and RX pair, in order to establish a robust communication, should configure their BF radio interfaces looking for the best combination of directional beams all over the entire space. As proposed in literature in [31 - 35] and in standard [10 - 12], one basic point is the use of discrete digital Beamforming, with DFT-based codebook: a set of orthogonal patterns, done by orthogonal weights, are collected in a collection called codebook, then they are used to scan sequentially the communication space. The entire multistage mechanism can be included in a predetermined protocol, shared obviously by all terminals, that will be run on demand or pro-actively depending on the possible propagation scenario and network topology. In details, recalling for simplicity the ULA case, we compute M orthogonal weights vectors and gather them column by column into a matrix  $\mathbf{W}$ . The integer index 'm' goes from  $-M/2$  to  $+M/2$ . Then we generate the M relative beam patterns with equal amplitude or gain. Each of them has a beam maximum at  $\theta_m$  and the entire set cover all the  $\theta$  angle domain.  $\mathbf{X}$  and  $\mathbf{Y}$  are simple input and output data vectors for the codebook weighting process:

$$\begin{pmatrix} y_0 \\ \vdots \\ y_{N-1} \end{pmatrix} = \begin{pmatrix} \mathbf{w}_{-M/2}^0 & \cdots & \mathbf{w}_{+M/2}^0 \\ \vdots & \cdots & \vdots \\ \mathbf{w}_{-M/2}^{N-1} & \cdots & \mathbf{w}_{+M/2}^{N-1} \end{pmatrix} \begin{pmatrix} x_0 \\ \vdots \\ x_{N-1} \end{pmatrix}. \quad [25]$$

$$\mathbf{Y} = \mathbf{W} \cdot \mathbf{X}. \quad [26]$$

The orthogonality holds in this way and the m-th array factor is given by :

$$\int_{-1}^{+1} F_i(u) \cdot F_j^c(u) du = \mathbf{w}_i^T \cdot \mathbf{1} \cdot \mathbf{w}_j = 0 ; \quad \forall i \neq j. \quad [27]$$

$$m = -M/2, \dots, +M/2; \quad m \in \mathbb{Z}$$

$$\text{calling: } \theta_m = \arccos\left(\frac{2m}{M}\right);$$

$$F_m(\theta) = \frac{1}{M} \cdot \frac{\sin(\pi[\cos(\theta) - \cos(\theta_m)]M/2)}{\sin(\pi[\cos(\theta) - \cos(\theta_m)]/2)}. \quad [28]$$

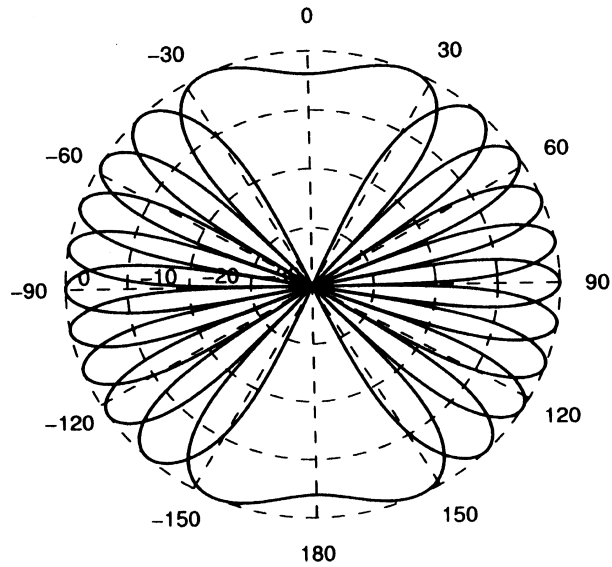


Fig.30: all codebook patterns in a  $\theta$  polar plots.

In the 802.15.3c standard [10], the beam searching is done in an intuitive way: the candidate BF weights vectors are listed in a codebook and are tested one by one in an exhaustive way. The BF combining pair which offers the highest signal-to-noise-ratio (SINR) is chosen for the signal transmission. To accelerate the process, the beam searching is divided into 2 phases: in the first phase, an antenna diagram with a wide main lobe -so called “sector”- is used for a fast and preliminary estimation, whereas in the second phase an antenna diagram with a thin main lobe and high gain -so called “beam”- is applied for precise estimation within the range of the rough estimation. The other terminal in every phase is set in a quasi-omni pattern configuration and plays a passive role just recording the right power information for each tried beam.

## Beamforming Terminology

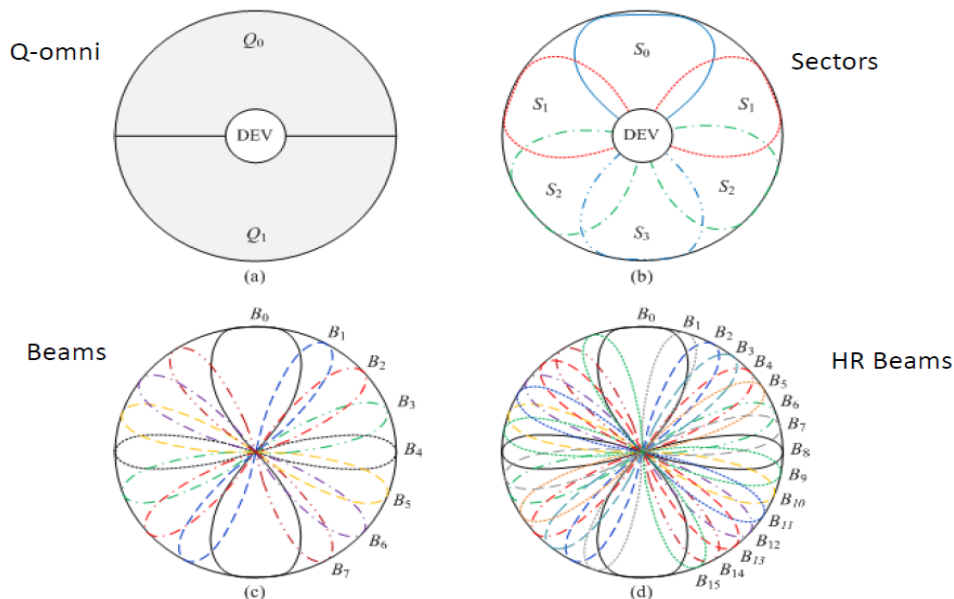


Fig.31: common BF Searching terminology.

The Beamforming training procedure in IEEE 802.11ad draft standard [12], similarly, advocates three steps: sector level sweep (SLS) for the TX with quasi-omni receive pattern, the multiple sector ID (MID) for the RX with quasi-omni transmit pattern, and an iterative beam combining (BC) algorithm for the best beams pair using subsequent data communications.

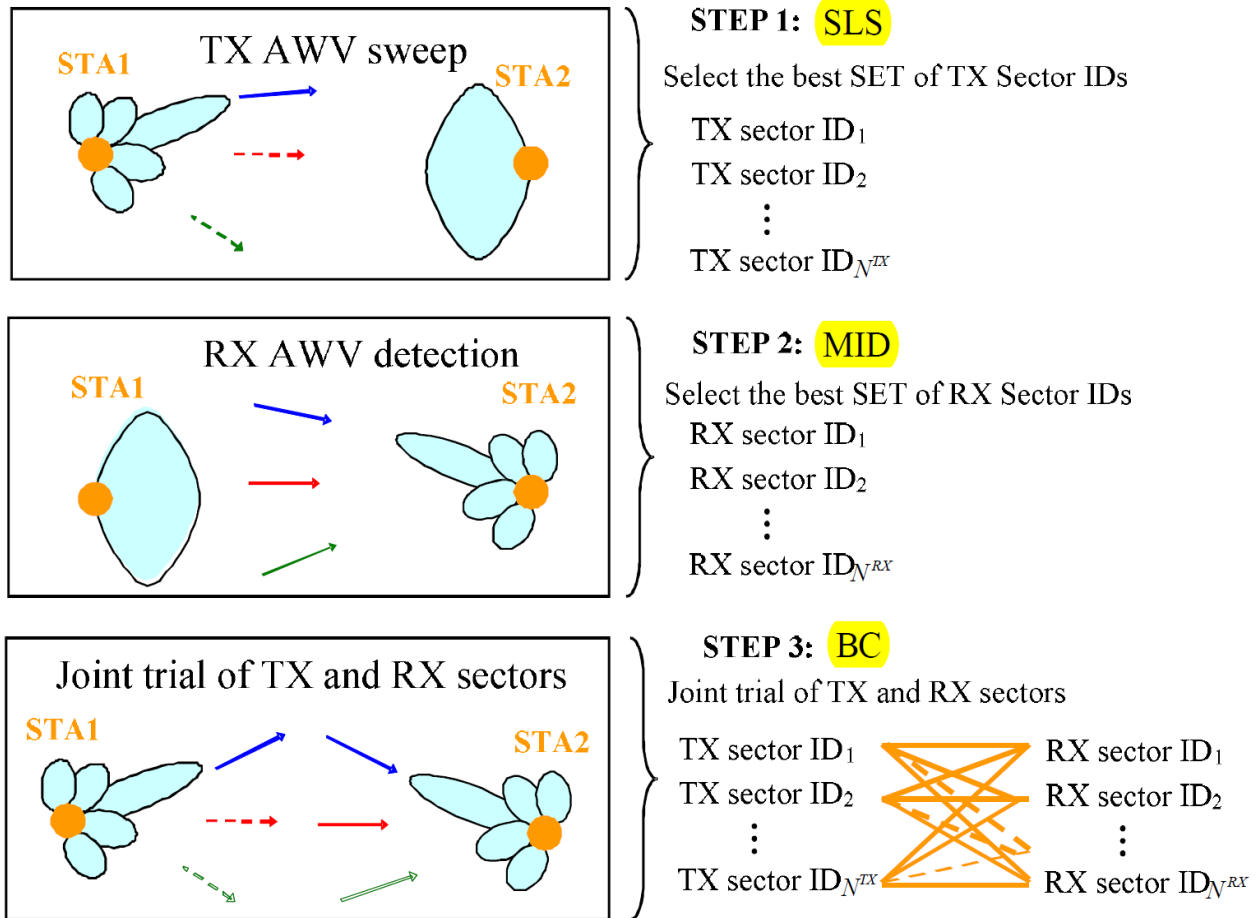


Fig.32: 802.11ad BF Searching protocol.

Taking as example the already cited article in [14] we deal with two sets of 30 GHz mmWave Beamforming prototypes that play the roles of a base station and a mobile station. Here the 2 channels 8x4 sub-arrays URA antennas used, (Fig.33), are able to provide 18 dBi of gain and a HPBW equal to 10° in azimuth and 20° in elevation.

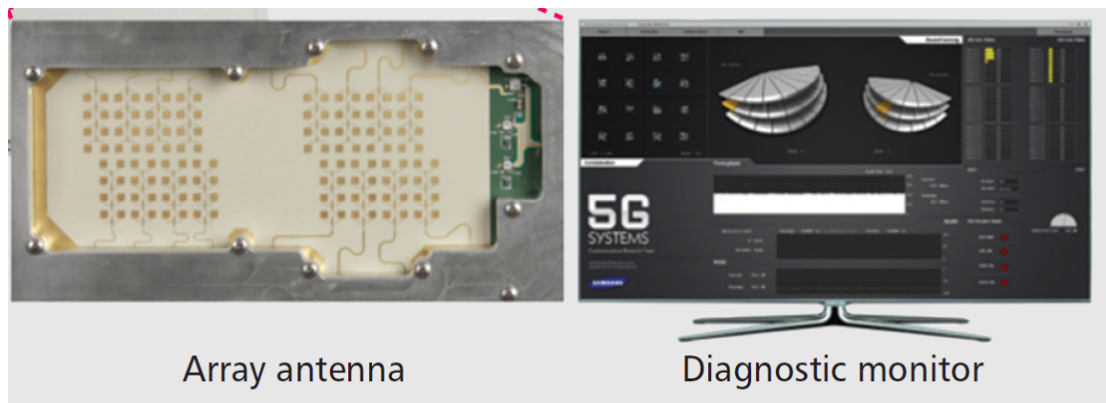


Fig.33: Samsung 30GHz BF multi-antenna prototype.

The defined Beam Searching protocol is again similar to the standards ones but lighter: for the downlink transmission, the base station periodically transmits a sequence of measurement signals in predefined beams so that the mobile station can carry out, also in predefined receive beams, channel quality measurements of the transmit-receive beam pairs. Then the best relative beam ID is fed back to the base station for the subsequent downlink transmission until the next update. In this fashion, the base and mobile stations establish the wireless communications link and could adaptively sustain it. The communications link setup for the uplink is done in an analogous way where the roles of the base station and mobile stations are interchanged. The developed mmWave BF prototypes are able to complete the search for the best transmit and receive beam pair within actually 45 milliseconds. Considering the PHY layer with OFDM frames as in [36][37] and [12] a time interval of  $\sim 50$  msec could be too large in practice, especially in case of high mobility or in dense urban environment where channel fluctuations are fast. Nevertheless focusing on indoor scenarios, like homes or offices, we know that propagation is somehow limited by the environment and the mobility is approximately negligible, so Beam Searching can be faster and easier. Also in this case a rough evaluation of the necessary total time is not trivial because it is strictly related to BF architectures and no rigorous information about it has been published yet. Therefore we shall think about different solutions: smart BF terminals could store automatically the localization information creating a database of the users positions and routes. Just think about a very usual case where the access point is fixed on the wall and the user is working with its laptop on a desk. An other valid alternative, as totally discussed in the following chapter, can be offered by Ray Tracing method that is able to provide directly the right AoA information, without any expensive “blind” research or protocols, as discussed in the following chapter. In the end the results of the Samsung study in [14] show promising general performance for this kind of novel wireless communications. For example a range of 1.7 km for outdoor LOS link -with negligible block error rate (BLER) below  $1e-6$  and EIRP equal to 49 dBm- has been achieved. By the way in case of NLOS sites or outdoor-to-indoor penetration cases, the link quality can be very poor and so coverage holes may occur, (Fig.34):

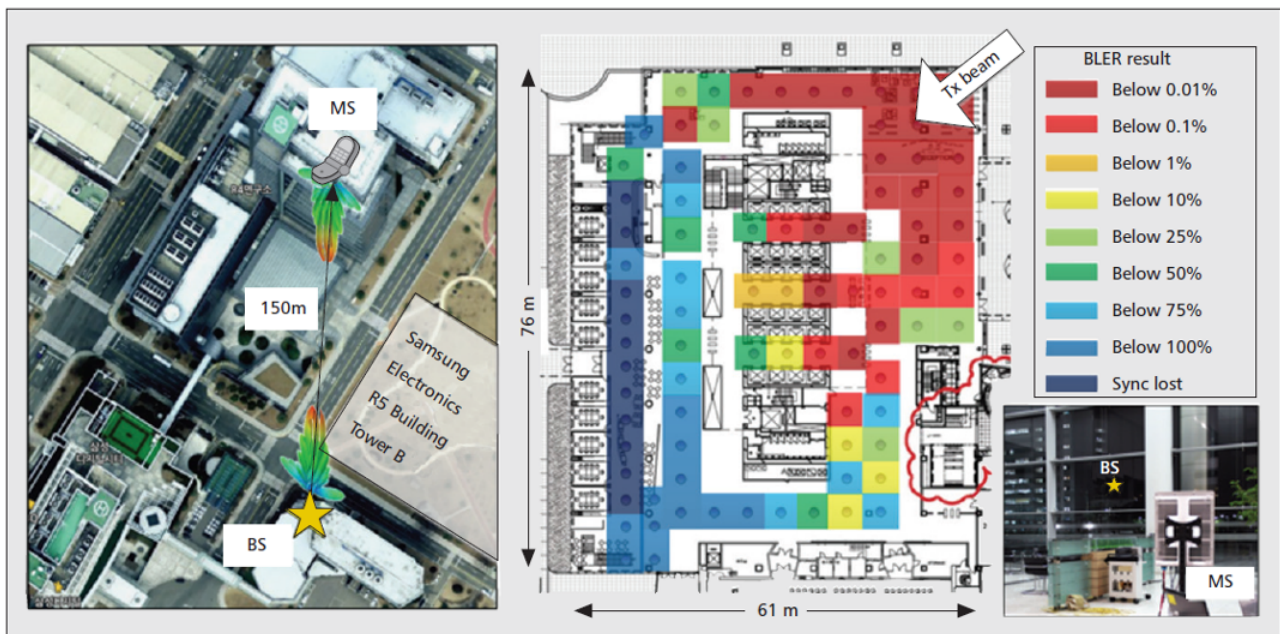


Fig.34: outdoor-to-indoor example of link quality.

For sake of generality, Beam Searching issue regards also the MAC layer because of the usual necessary messaging during any kind of protocol dialogue. The traditional MAC protocols, as the well-known CSMA, typically fail to exploit the potential benefits of BF multi-antenna system, particularly in ad-hoc ever-changing networks, simply because they were designed originally to run on omni-directional devices. In [38] there is the whole discussion, we just outline (Fig.35) a

literature proposals summary:

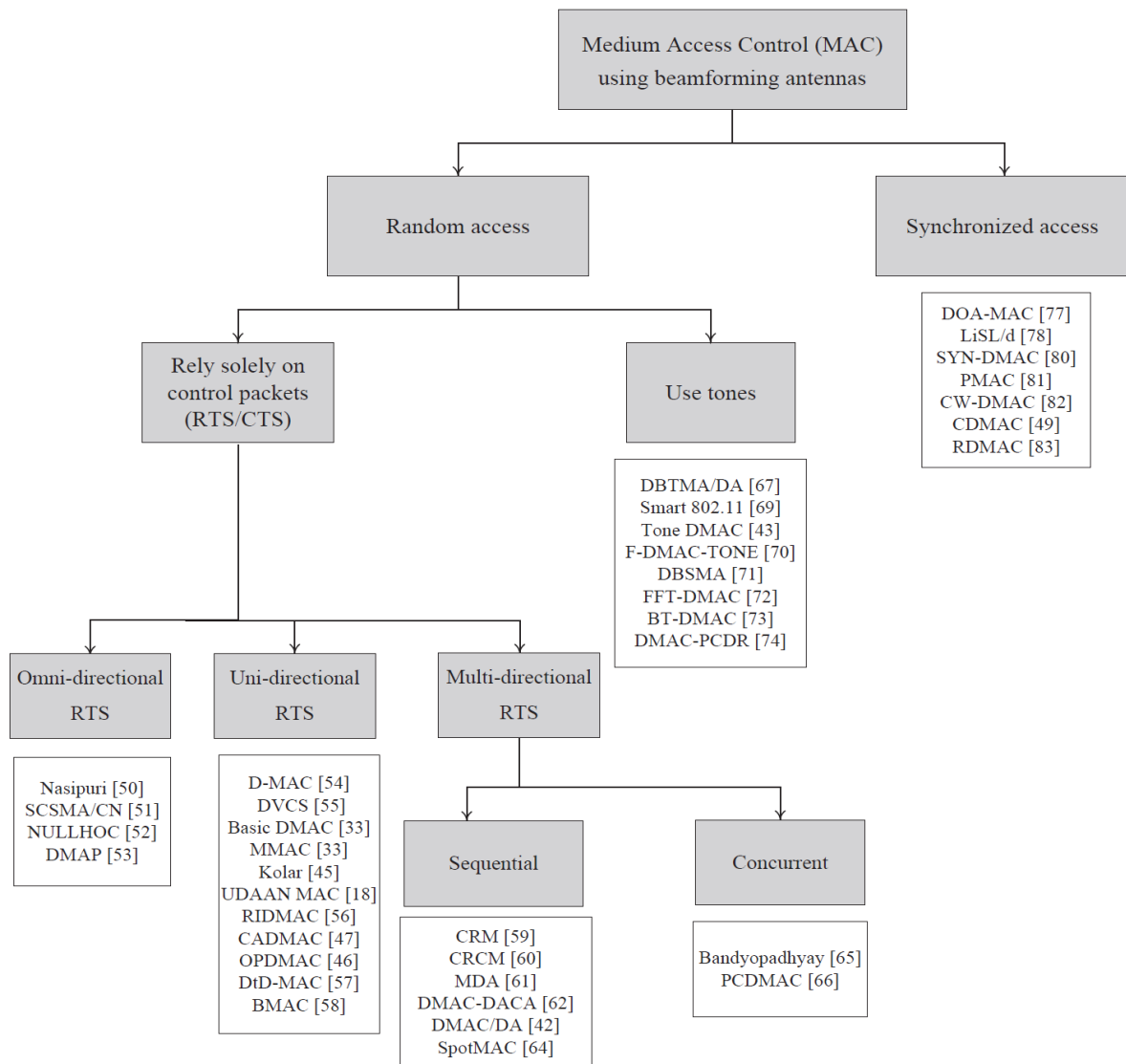


Fig.35: a taxonomy of the possible directional MAC protocols.

# Ray Tracing:

## 1) General Description

Ray Tracing (RT) is a powerful deterministic numerical method used to study and forecast the radio channel in a given propagation scenario. Differently from electromagnetic simulations based on Maxwell equations like MoM, FEM or FDTD, the RT is based on the well-known Ray concept developed in classical Geometrical Theory of Propagation (GTP), in modern Geometrical Optics (GO) and also in Uniform Theory of Diffraction (UTD) theories. Nowadays Diffuse Scattering (DS), using for example the Effective Roughness (ER) [39 - 43], is often included in the whole framework too, such that all electromagnetic waves phenomena can be mathematically gathered and described as well. RT model requires a detailed and complete description of the environment as input data, both geometrically and electromagnetically: a 2D or 3D scenario map, indoor or outdoor, and the entire set of e.m. parameters of the objects or buildings that surround the antennas systems. Collecting all this information, to re-create the propagation space in simulation, may be hard and it represents indeed the main cost of the process. The usual presence of compound materials or unknown unhomogeneities may lead to serious hindrances for a reliable RT assessment, and therefore a limit to the final prediction accuracy.

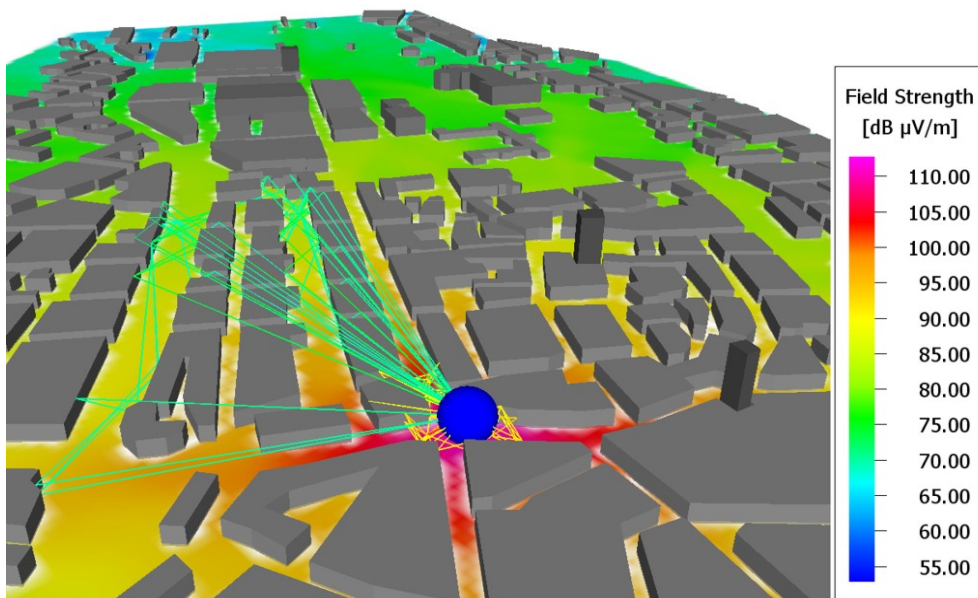


Fig.36: typical Ray Tracing simulation.

RT can be implemented in different ways. Taking as reference the RT software named 3DScat -developed at the University of Bologna by the group of research in electromagnetic propagation and wireless channel modeling- we can spot two main stages: the view tree construction, where iteratively the RT, on the basis of the visibility concept, discovers the existence of radio propagation paths between the transmitter and the receiver, and then the back-tracking procedure, where the RT determines the exact interactions and trajectories of the rays. At the end, the complete e.m. field at receiver side is calculated from previous rays results. Eventually using the equivalent circuit model and knowing the antennas properties, other useful outputs as received power, delay spread, coherence bandwidth, angular spread and AoA/AoD can be obtained too. Although RT is intrinsically site specific and deterministic, it can be indeed exploited to provide a statistical characterization of different, representative scenarios. In fact, multiple RT runs can be carried out inside the same environment, and the results can be collected and regarded as different realizations of the same random process. Therefore, statistical parameters such as mean values, standard

deviations, cumulative distribution functions (CDF), correlations can be computed as well. For instance, with reference to a MIMO systems affected by correlated Rayleigh or Rice fading, the RT-based statistical characterization can include important CSI as the Rice factor (K) and the complex correlation coefficients at the TX/RX sides. Due to its intrinsic 3D computational burden, every time RT is launched we must cope with the trade-off between prediction accuracy and processing time, according to the number and the type of possible interactions assigned to each ray. Unfortunately, considering the complex and various nature of the propagation scenarios, especially in outdoor, this drawback can restrict dramatically the RT performance. By the way experimenting the RT with modern powerful computing architectures -for example parallel computing, cloud or grid computing or even GP-GPU processors, as well as it happens in computer graphics engines for visual effects rendering- could in the next years make the RT very suitable and easy to use, with considerable reduction in computational time compared to the past years. Today RT, anyway, represents the unique simulation tool able to achieve precious information about multipath and wideband channels, without any kind of measurements or sounding, and so practically it is perfect, unlike traditional Hata-like or other empirical models, to design and deployment the actual mobile networks, for example 4G or WiFi. Making a step further, as shown in [44 - 48], we can also point the utilization of RT at mm-Wave out. We know that the optical approximation of the definition of Ray is still right and even more precise due to small wavelength, but all the laws of interactions, that rule the propagation, might be misunderstood and badly interpreted, thinking in terms of UHF frequencies. Therefore new studies and new RT versions for mm-Waves are becoming today very crucial. When a radio wave impinges actually on a building wall the field is scattered in a wide range of directions, due to rough surfaces, decorative masonry and inner irregularities -such as inner reinforcements, power lines or heating pipes doors- and external irregularities -as windows, rain pipes, picture frames, windowsills and balconies-. Thus the complex permittivity  $\epsilon_c$  of the examined wall may vary in frequency in an unknown dispersive way. So at the end its response may change radically with respect to its well known UHF characterization. The strong sensitivity of RT models to the accuracy in the environment description can represent in fact a big problem at millimeter waves, since only a few studies, as [49][50], on the characterization of the EM properties of materials in the millimeter-wave bands, are available in the scientific literature up to date.

Moreover focusing on the surface roughness at mm-Waves, DS can not be neglected because of the new relationship between objects dimension and the operating wavelength. According to the approach in [39 - 43], scattering from a finite surface element is regarded as a “diffuse phenomenon”, and so it can not be reduced to few contributions coming from specific interaction points -like reflection, diffraction and transmission- but on the contrary it rather springs out from the whole surface illuminated by the incoming wave. This all means, as rule of thumb, that essentially big obstacles could produce much more scattering contributions and, also, that small obstacles could produce more reflection contributions, at the expense of the diffraction ones. Thus one of the major open issues today concern the role of diffuse scattering at mm-wave frequencies with respect to common reflection/refraction: the key problem, under an heated debate, regards the search for the right ratio between Distributed multipath components and Specular components, with respect to UHF frequencies, (Fig.37).

## ***2) Real Time Ray Tracing***

Aware of the practical limits and future improvements, RT can be considered not only a prediction tool or a simple simulator, but a real-time asset for the wireless communications. We can imagine to use RT as an embedded software in the TX/RX chipsets able to provide reliable CSI and speed the overall MIMO algorithms up. As in [51], this idea can be called “embedded Ray Tracing” or “Real Time Ray Tracing”. In case of Beamforming, as already said before, the use of RT can improve significantly the AoA/AoD estimation or the Beam Searching and Tracking protocol once the propagation scenario has been digitized and electromagnetically analyzed.



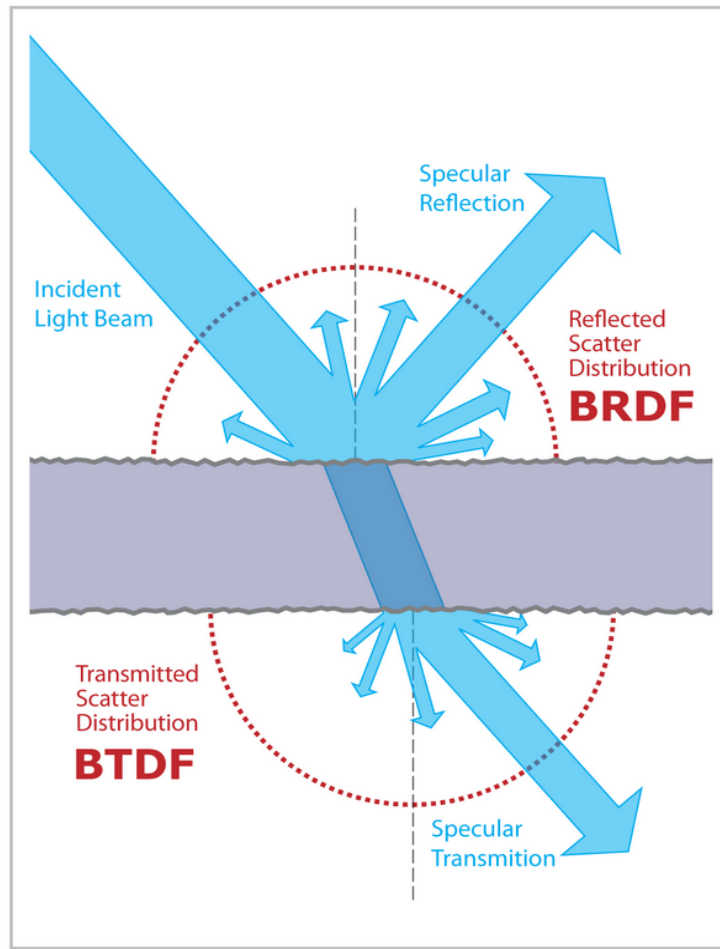


*Fig.37: Reflections and Scattering of a light beam.*

We know that the execution time required by a codebook-based BF algorithm, depends on the codebook size and can become quite large when beams are very narrow and/or a beam scanning over a wide 3D range is pursued. Moreover irrespective of the specific implementation, a codebook-based beam tracking algorithm can be expected to perform well in static condition, where it should be likely run just once as the radio link is set up. On the contrary, some doubts may arise about its effectiveness in a time variant channel. For instance, in large and crowded scenarios where moving people or other moving objects may suddenly block the radio, the tracking algorithm should be run over and over again, to the detriment of the overall system performance. Then it is worth noticing that RT-based beam searching could naturally cope with fast and sudden channel changes (e.g. abrupt human blockage), because once the stronger paths have been tracked by the RT engine, their AoD could be easily stored, so that the beams could be quickly re-arranged if needed. Recalling the results in [14] and protocols in [10-12] previously seen, RT-assisted BF could be even faster than standard BF solutions, provided that the paths tracking time in the RT tool is lower than -or at least comparable to- the average time interval necessary to complete the exhaustive search inside the codebook. It is not easy, as already outlined, to define an exact speed comparison, but we suppose that the required computation time would be reasonably small -in the order of few msec- in case of some RT simulations carried out in the small office environment where mm-wave channel is basically LOS or quasi LOS and so only few dominant, reflected paths can be considered.

# Ray Tracing based mm-wave Beamforming assessment:

## 1) Study Case

As previously discussed, a valid mm-wave radio channel prediction model like Ray Tracing is a very suitable tool to investigate different schemes of BF performance. Therefore an indoor study case using 60 GHz mm-waves on the basis of the following environment has been carried out, (Fig.38):

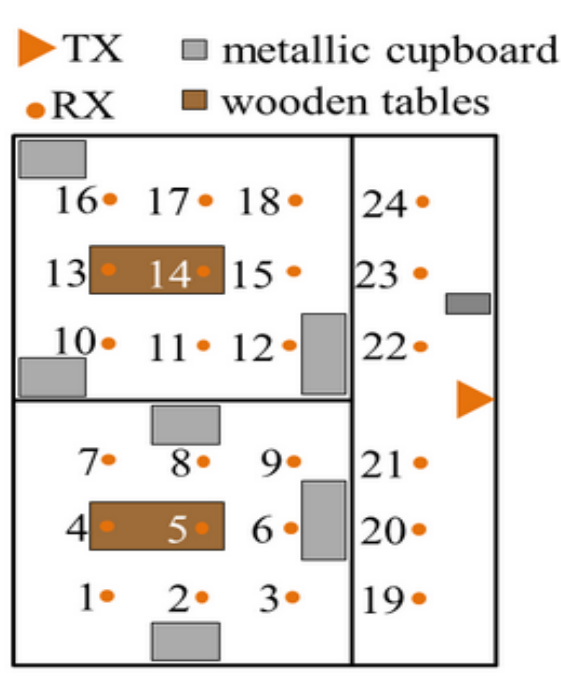


Fig.38: indoor offices scenario.

We have two adjacent offices with metal boxes placed close to the walls and wood large tables in the middle of the rooms. There is an additional metal cabinet in the corridor that is on the right of the scenario. Assuming this possible scenario for WiGig for instance, the TX is thought to be an Access Point and so is located on the right wall at the center of the corridor, whereas the 24 RX points are distributed uniformly in the rooms space. The entire floor is roughly 3 meters high and the TX is a meter and a half above the RXs. Respectively the TX is equipped with a 12x12 planar patch array antenna, able to make BF, using the Dolph-Chebyshev synthesis, with more than 20 dB of D whereas the RXs are only ideal isotropic terminals. This sort of asymmetry is of course a limit of performance but it represents anyway a realistic mm-wave link case nowadays in terms of cost and feasibility. The entire investigation has been carried out in Matlab simulations with the support of the already cited 3DScat RT program. The basic assumptions of the project are that the TX knows exactly the right position of each RX with the total awareness of the propagation environment. As already outlined previously, we know that these cases can be considered genie-aided and they do not mirror the reality -just think about the today WiFi-. Furthermore the RT configuration and e.m. parameters included in simulations are considered the ones at best tuned for 60GHz propagation, differently from common UHF bands, but no absolute certainties can be taken for granted today. The main goal is to find the best Beamforming scheme, in agreement with the Ray Tracing channel predictions, that is able to provide the maximum Carrier to Interference and Noise Power Ratios. Not using signals but only pure 60 GHz tones, we do not deal with bandwidth and so that is why the performance metric is simply the CINR. We choose three fundamental cases of RT assisted BF:

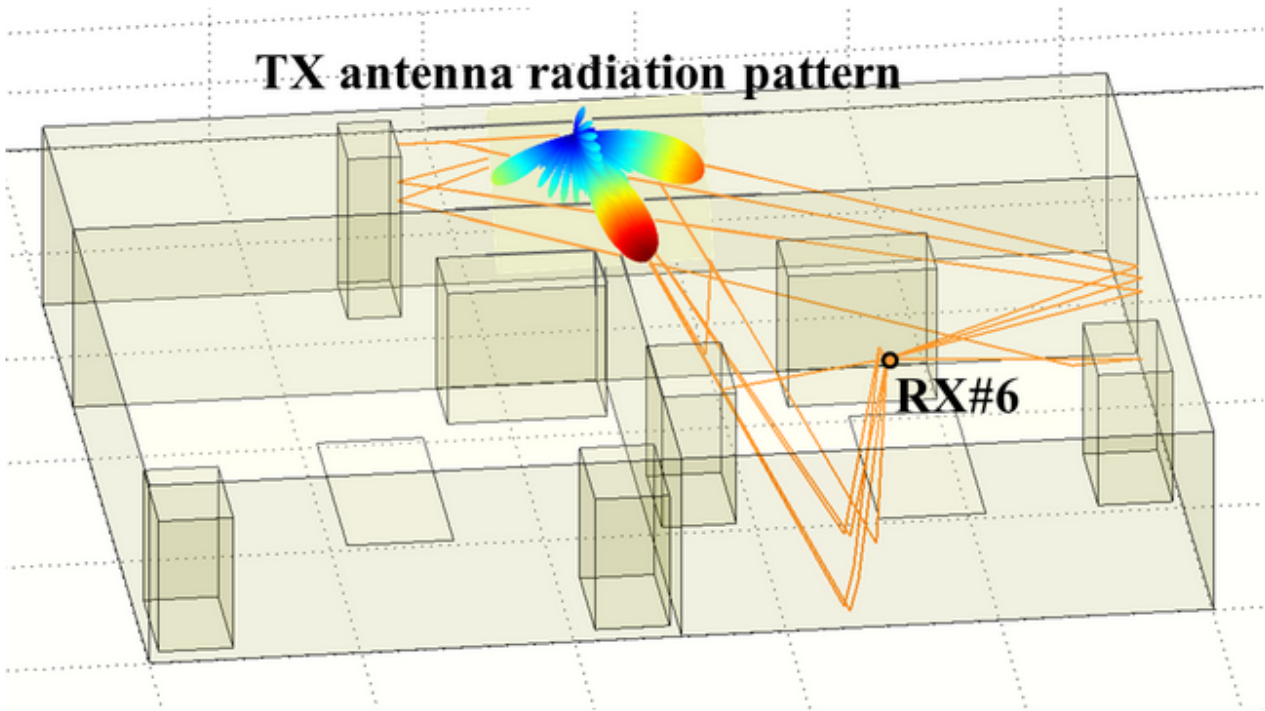


Fig.39: RT assisted BF 3D example.

**1 – Radial Beamforming:** the TX ignores walls and obstacles and so synthesizes the BF pattern directly towards the RX points. This is not a smart solution trivially, because the RT does not support the decision process. This case is used only as reference and can be considered a sort of localization assisted Beamforming. It is simple to see (Fig.40) that all the power transmitted will be wasted against the metal box that shadows the RX number 6:

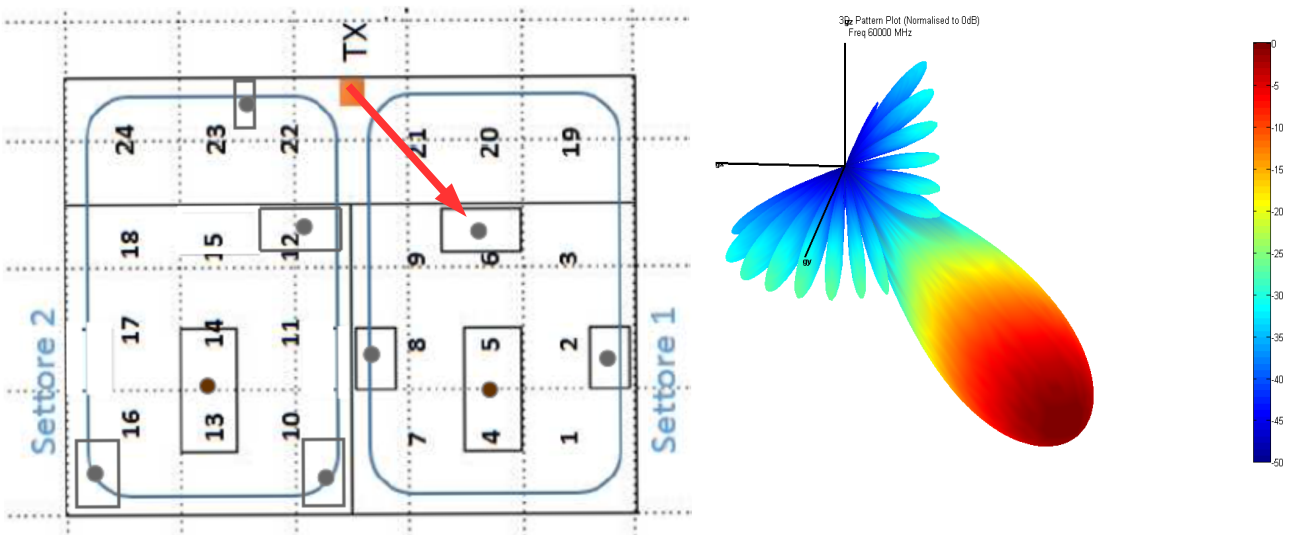


Fig.40: Radial BF case for RX 6 in NLOS on the left; Normalized gain pattern in dB on the right.

**2 – Single-beam Beamforming:** the RT considers initially the TX as an isotropic antenna, launch the simulation with all the scenario details and then provides the information about the rays: powers, trajectories, delays, AoA/AoD, number and kind of propagation effects ecc... The TX knows everything about the channel in this deterministic way and so is able to select easily the

optimal AoD where to apply the BF routine. That is why it is called Single-beam BF. We realize (Fig.41) that the TX has steered in fact the beam towards a direction far from the metal box:

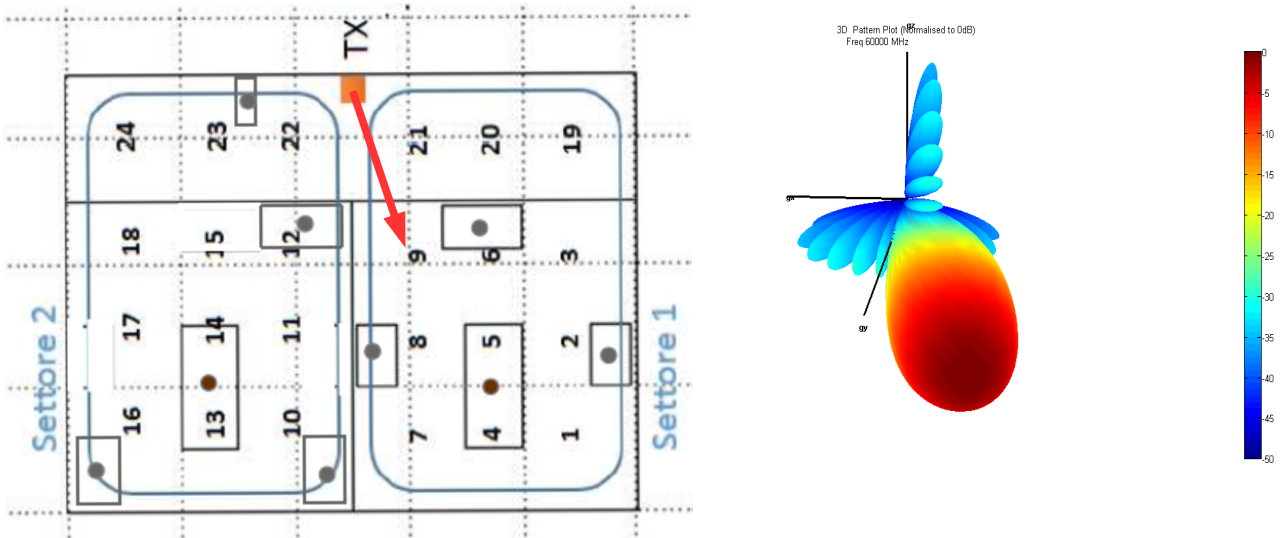


Fig.41: Single-beam BF case for RX 6 on the left; Normalized gain pattern in dB on the right.

**3 – Multi-beams Beamforming:** otherwise in case of mobility, as in crowded places, we can think to exploit the spatial diversity adding a sort of artificial multipath richness to the communication in order to circumvent possible blockages or link drops, as well as it happens in SDMA but with only one user in this case. The TX, as in Single-beam BF, retrieves the rays information from RT but in this case chooses, according to a predetermined numbers -called Beams Order (BO)-, a set of best rays. We assume that the TX could manage more than one beam and so more than one pattern at the same time. Thanks to linear properties of array factors, as seen before, the TX makes the BF towards each AoD a number of times equal to BO and then sums all the array factors functions together before transmitting. The result at the end is an overall pattern with multiple beams that point to different directions, covering more spaces and creating more paths. For example if some rays belonging to one specific beam are stopped along the path by a walking person, all the other ones, that follow different propagation routes, could somehow sustain the link quality avoiding dramatic power drops and reducing the whole outage probability. Of course the price to pay is less directivity in principle. We can see (Fig.42) the multiple beams pattern with Beams Order equal to 4:

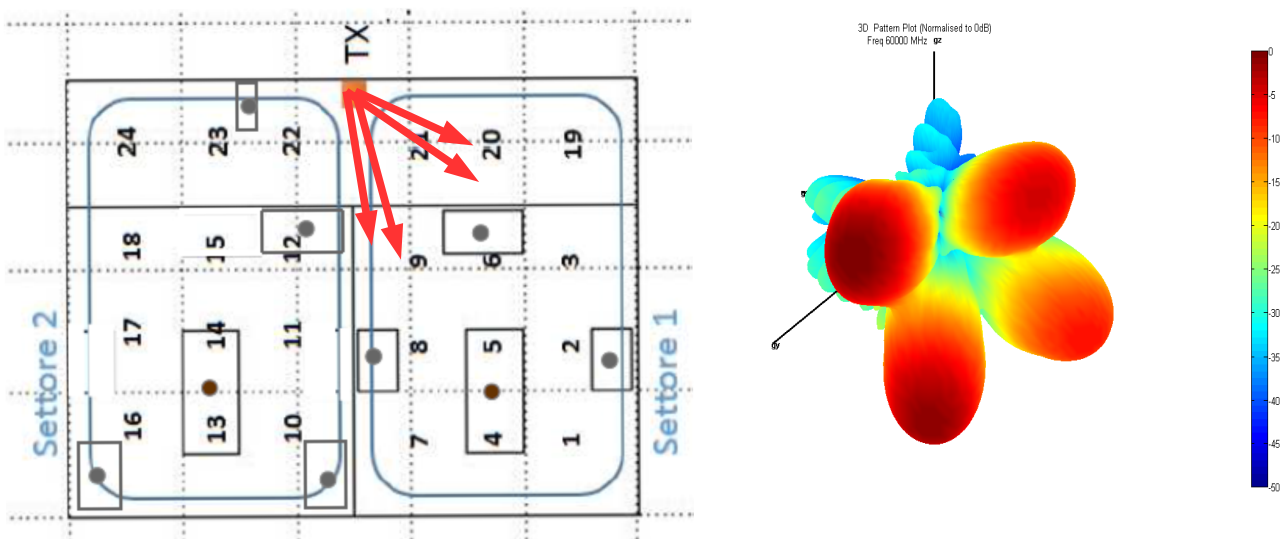


Fig.42: Multi-beams BF case for RX 6 on the left; Normalized gain pattern in dB on the right.

Once the TX has found and applied the right BF configuration for each RX, for every BF schemes, finally the RT is called again playing the role of channel prediction model in order to achieve the performance results in terms of CINR. The comparison among the different cases has been done according to the EIRP limit -equal to 40dBm- for Europe at 60GHz mm-wave band as defined in [52][53] and by IEEE too. This means moreover that the Multi-beams BF can compensate its directivity handicap, with respect to the Single-beam case, just using more power at TX and viceversa the Single-beam BF can save energy due to its large gain pattern, as shown in the following equation:

$$P_{TX}[\text{dBm}] = \text{EIRP}[\text{dBm}] - D[\text{dB}]. \quad [29]$$

In this kind of evaluation for sake of simplicity the CINR values have been obtained assuming the AWGN noise fixed at a floor equal to -100 dBm/Hz and the interference created by only one interfering user, located at one of 24 RX positions in the scenario. The final CINR value for one RX is then the average of the 23 single CINRs given by each pair formed by that RX and all the other ones, as in the following equation:

$$\text{meanCINR}_i = \sum_{k \neq i; k=1}^{23} 10 \log_{10} \left[ \frac{C_i}{(I_k + N)} \right]. \quad [30]$$

Regarding the useful power carried by the 60GHz carrier and also the other interference powers, they have been computed considering the basic antenna equivalent circuit, (Fig.43):

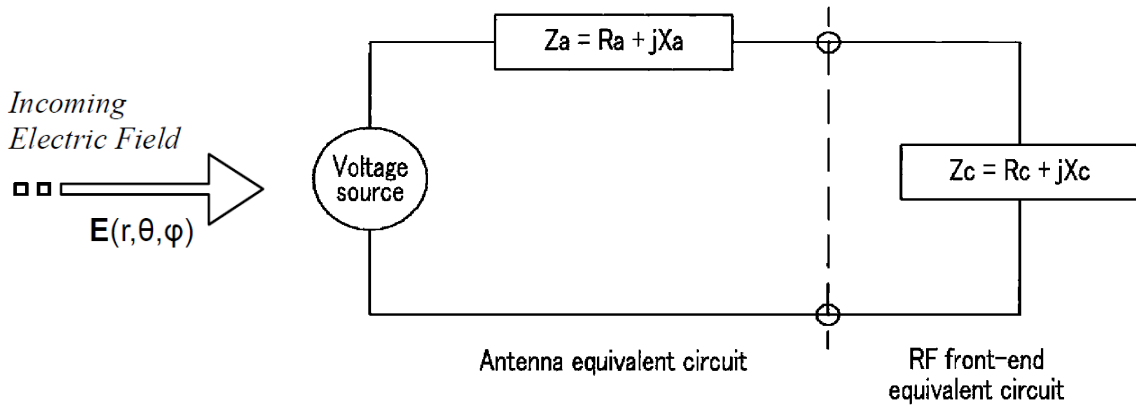


Fig.43: Equivalent antenna circuit.

Assuming the isotropic receiving antenna perfectly matched both in impedance and in polarization, -this a very lucky case in reality- there exists a proportional relationship between voltage and incident electric field that leads immediately to electric power definition, as follows:

$$V_{\text{source}}(\mathbf{E}) = \mathbf{y} \cdot \mathbf{E}(r, \theta, \phi). \quad [31]$$

$$\text{Pow} = |V_{\text{source}}(\mathbf{E})|^2 / (8R_c). \quad [32]$$

## 2) Multi-Beam BF

Multi-beams BF could improve significantly the robustness of the wireless link and RT, as we have already seen, is its optimal natural enabler. The availability of multiple beams opens more degrees of freedom in the BF procedure because each beam -that belongs to a specific radiating pattern related to a selected AoD of the rays-, can be weighted with respect to the others. As shown in the following equation:

$$F_{\text{tot}} = \sum_{j=1}^{\text{BO}} (p_j \cdot F_j). \quad [33]$$

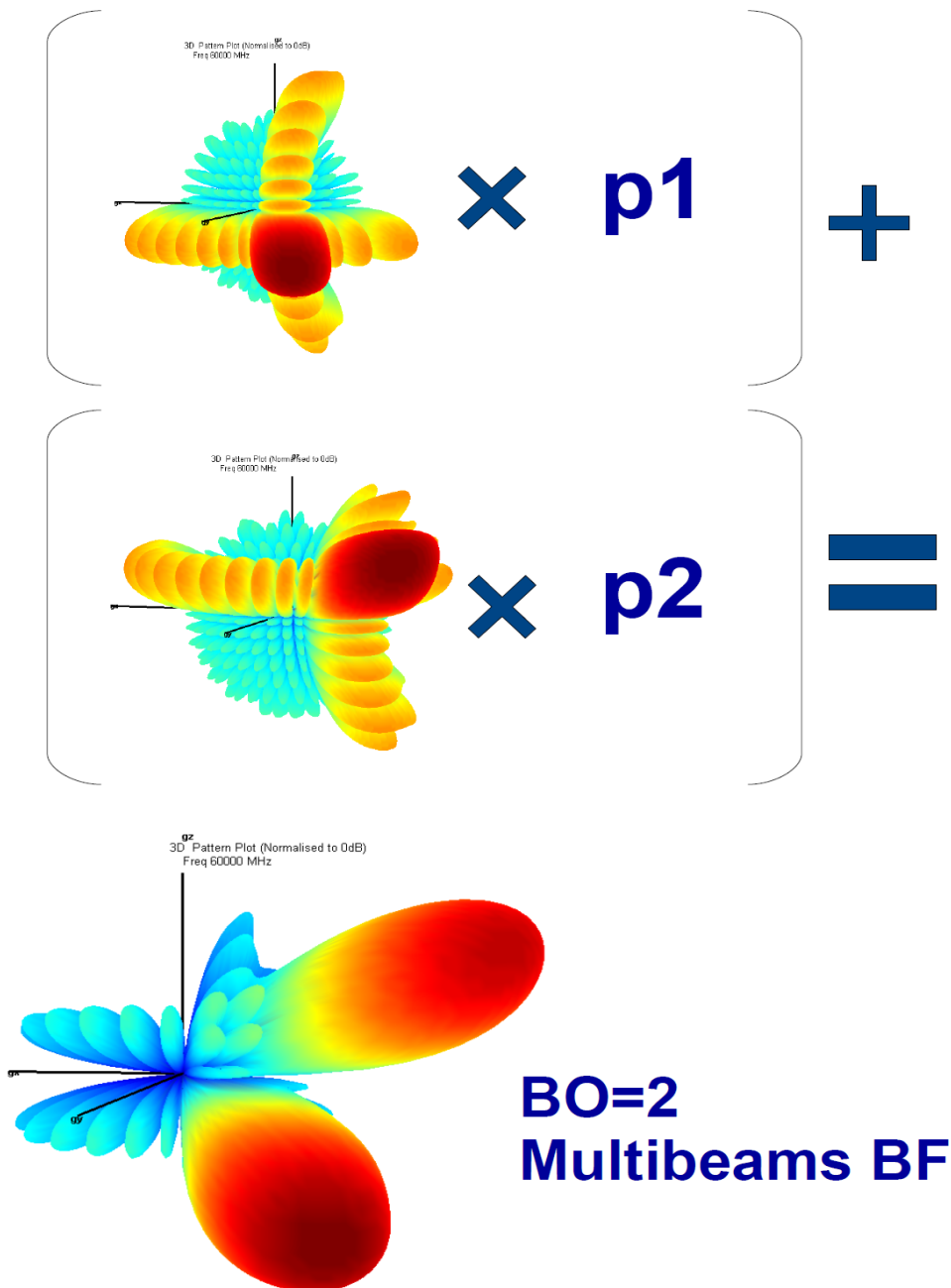


Fig.44: an example of 2 beams linear combination.

Each array factor can be shaped numerically by a scalar weight called  $p_j$ . We have a graphical example (Fig.44) of a 2 beams merged together with weights  $p_1$  and  $p_2$ . The final result is the complete array factor of the 12x12 patch antenna. As well as it happens in Maximal Ratio Combining scheme for RX diversity, we can choose to use weights that are extracted from the right ratio between the beam power -that is directly provided by the RT- and the total amount of power at TX, as it follows:

$$p_j = \sqrt{\frac{\text{Power}_j}{\text{Power}_{\text{total}}}}. \quad [34]$$

The trade-off behind the beams weighting is essentially given by the amount of spatial diversity desired to be carried out. For example if all the weights are unitary we obtain a BO numbers of beams with no imposed relative amplitude difference and so we achieve the maximum diversity in the spatial domain. Otherwise we can make some of the beams stronger or weaker with respect to the others, till reaching the extreme case where the Multi-beams BF degenerates into the Single-beam BF and so no diversity is involved.

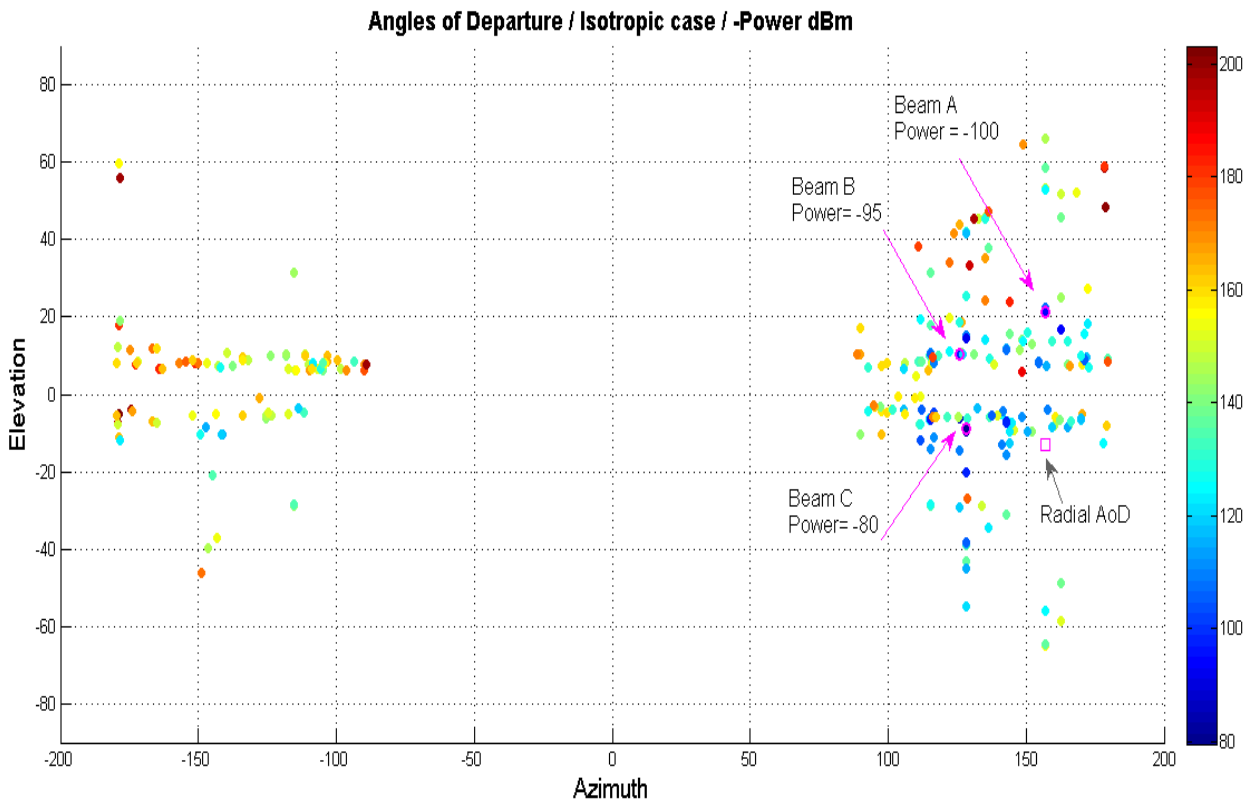


Fig.45: Angles of Departures for RX 13; Rays powers in dBm are expressed by colors.

Moreover RT assisted Multi-BF scheme is also suitable for a special a priori Equalization processing, because all the useful information about the channel are known at TX side -where RT tool is used in our case-. The starting point is already described and it can be visualized (Fig.45). After the RT simulation, TX selects the BO best AoDs and focus the power in these directions. Without any modifications of the signals, considering the RX side now, we have that the rays come from different AoAs but with different delays too, (Fig.46). The artificial multipath made by Multi-beams BF is indeed not completely under control in the time domain and so there is no constructive sum at receiver. In the study case scenario the room is 7x10x3 meters and so delays are small numbers in the order of nsec, but generally these kind of problem always regards wireless digital receiver architectures, especially in outdoor urban environments. -just think about ISI-.

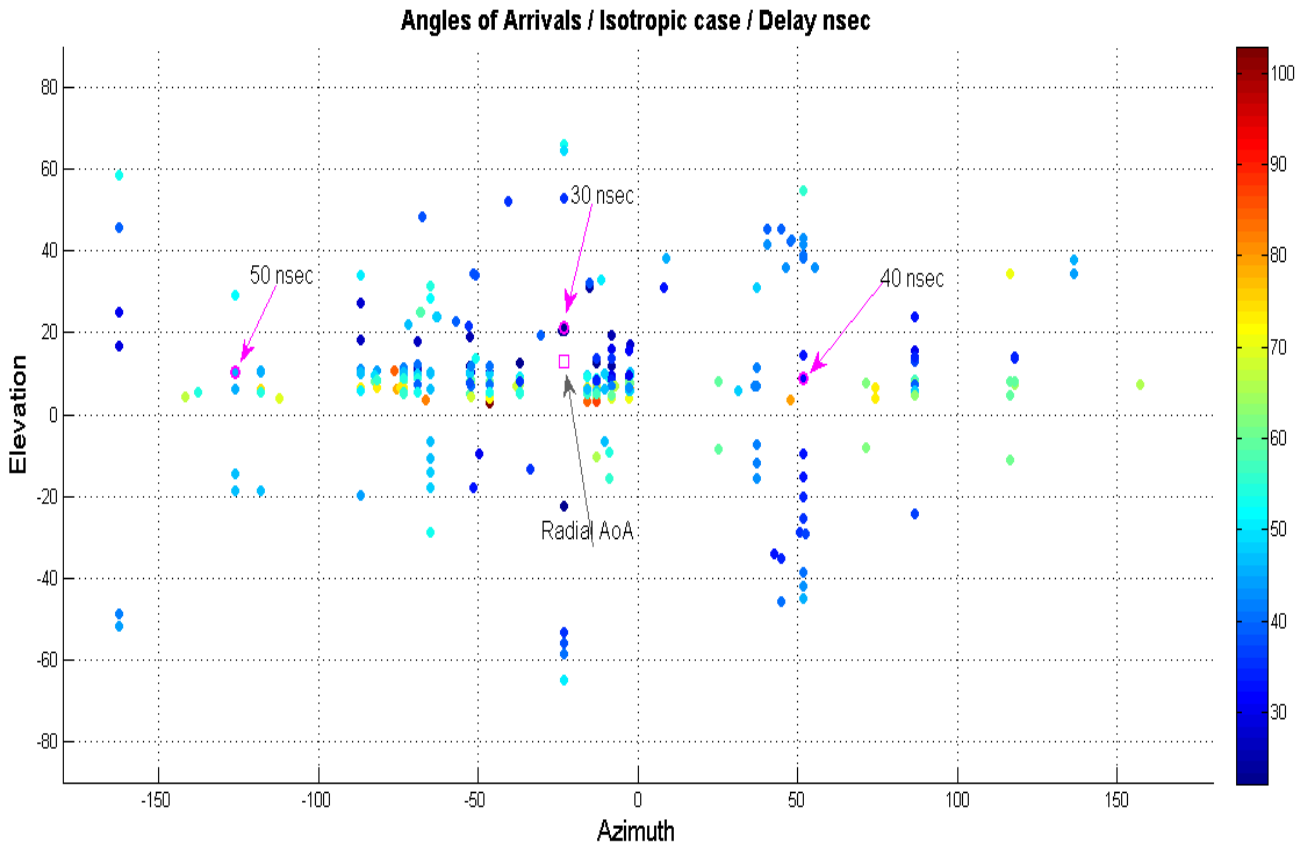


Fig.46: Angles of Arrivals for RX number 13; Propagation delays are expressed by colors.

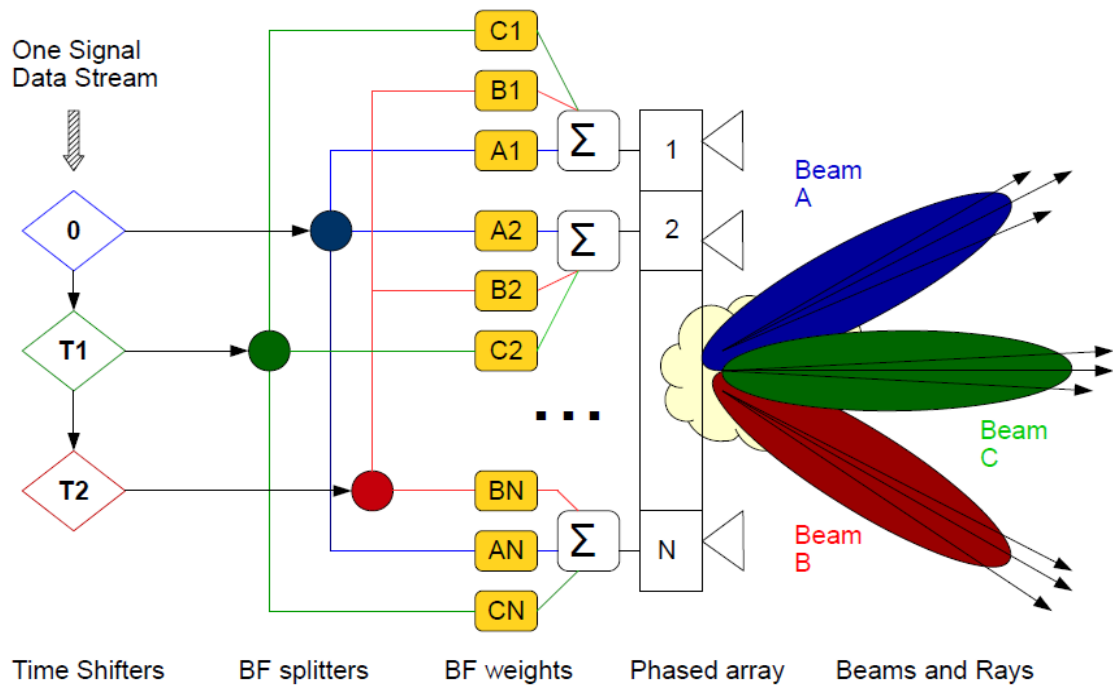


Fig.47: Space time BF block diagram; a priori Equalization at TX side.

To solve this issue the TX shall manage the signal in time sending different delayed versions of it into the Beamforming blocks such that all the rays inside the beams could arrive at the same time at



RX side. For example with BO equal to 3, (Fig.47), the TX orders the beams in terms of delays: The first beam, called A, that is related to the slowest rays -and of course to the longest paths- the second intermediate one, that is C, and in the end, the third one, called B, related to the fastest rays. Setting a precise clock and calculating the differences among the three beams rays delays the TX sends the signal in postponed instants waiting from one beam to the next one the exact corresponding time. This technique is a complete space-time processing strictly affiliated to the deterministic RT predictions and involves for sure a lot complexity. Furthermore it is possible to think about a more complete equalization that could take into account even the polarization where the polarization of the field emitted through the different beams can be similarly a priori set in order to provide a strong polarization efficiency at the RX.

In conclusion we need to discuss about the value of the parameter called Beams Order, that is the number of beams operated by the BF. In the study case, with respect to the kind of environment and assumptions made, we found that BO equal to 4 is already an inefficient solution because the available power is spread in too many direction, (Fig.48).

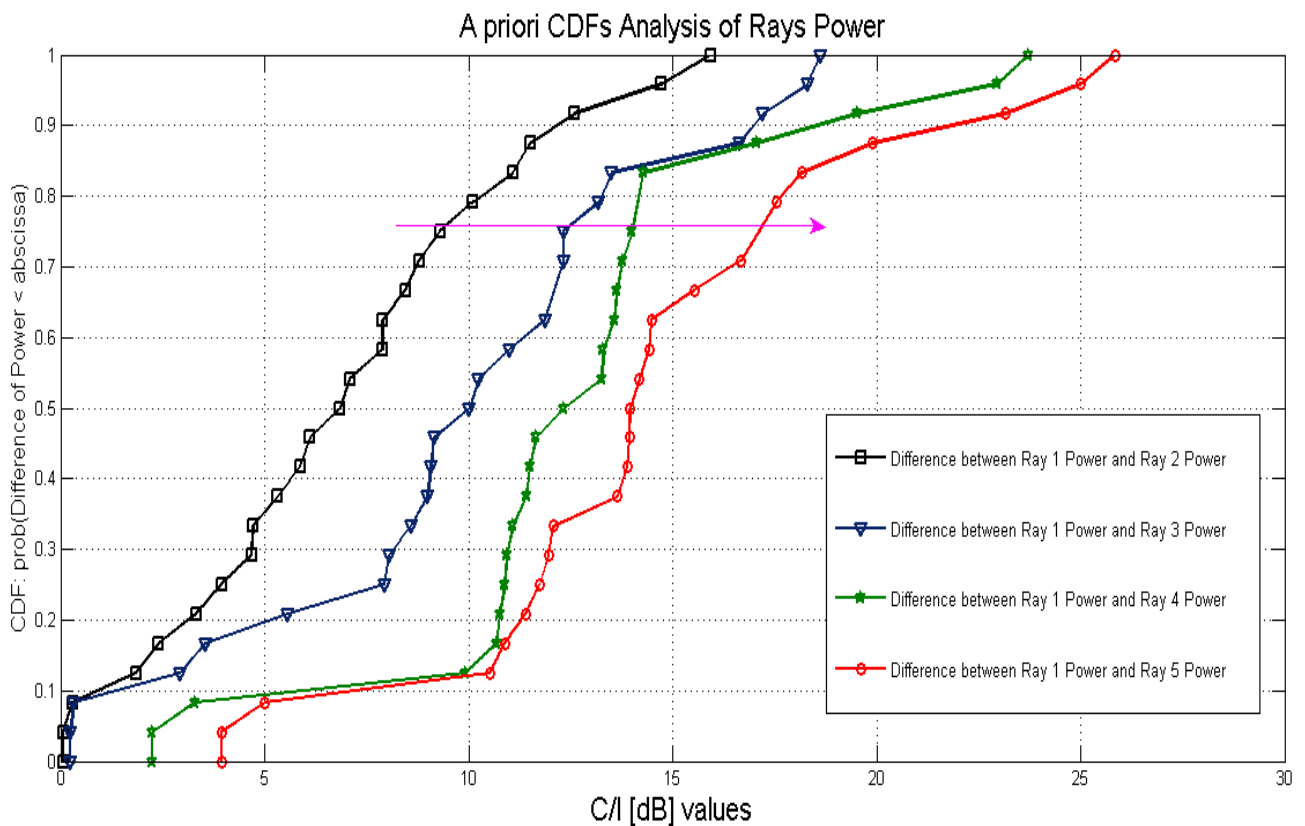


Fig.48: CDFs of rays power differences to explain the role of BO parameter.

Ordering the rays in terms of power and taking the first one as reference we can calculate the differences in dB and create the CDFs functions for all 24 RXs under examination. For the 80% of the rays we have 10 dB of power gap for the second ray, 12.5 dB for the third one, 14 dB for the fourth one and even 17.5 dB for the fifth one. This is just an example, but we know that propagation scenarios like indoor offices easily lead to dealing with a particular set of rays, where there is a clear strongest path and many others that can even have a 20 dB of power loss. This is the proof that the Beams Order, as rule of thumb, loses usefulness if greater than 3. Of course the BO is also upper bounded due to feasibility and complexity. In case of blockage and dynamic channel conditions, having a large BO can be instead a surprising advantage because, as already said, spatially separated alternative paths are anyway active. In the following results it has been assumed to be in the worst case where all the rays that follow the best paths and so are related to the biggest percentage of

power, are blocked and attenuated of 30 dB of power. This specific number has been taken from studies like [54] and [55], and represents a reasonable power drop caused by human body obstruction.

### 3) Results

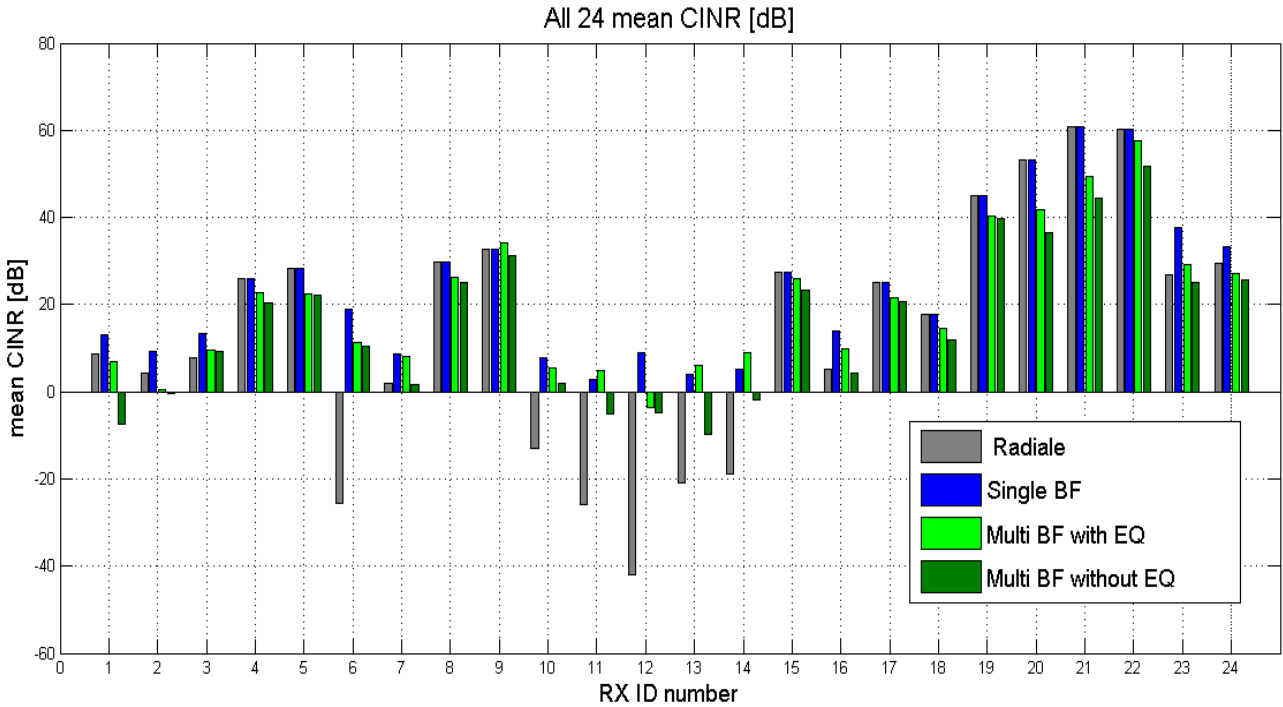


Fig.49: all mean CINR values for each RX.

It is evident (Fig.49), that Radial BF fails, as expected, each time strong NLOS conditions are present. For example in cases of RX numbers 6 and 12 the CINR mean values go beyond zero dB. In RXs from 19 to 22, instead, there are LOS and good proximity between TX and RX, so CINRs get high till 60 dB. Here Radial BF shares the same results with the Single-beam BF, because they are trivially identical. Better performance instead for Single-beam and Multi-beams BF, where the RT support is fundamental and increases significantly the useful received power. Since no Human Blockage and no Array Factor weighting are taken into account here, the best scheme globally seems to be at the end the Single-beam BF -just looking at RX number 12 again-. It is important moreover to underline the divergence between Multi-beams BF with and without equalization: in special cases like RX 13 and 14, the equalized Multi-beams BF is the best scheme, overcoming the Single one, and the unequalized Multi-beams BF instead has very bad negative CINR. Otherwise the gap between the two variations of on average is not so big.

Summing up we can have several discrimination factors for the special case of Multi-beams BF plots: with 2 or 4 beams as Beam Order -to see the differences of spatial diversity-, with or without a priori equalization -to see how much valid is this technique- and finally with or without Multi-beams weightings -to see the difference of beams power allocation in space-. We have the complete set of possibilities (Fig.50) with all the BF cases. Two general comments follow: with HB losses in the simulations the Multi-beams BF is able to strike the Single-beam BF. Without HB, but using the array factors weighting in Multi-beams BF, similarly to MCR algorithm, the results are slightly better because a smarter balance of power is chosen considering the free paths conditions where Single-beam BF is known to be the best scheme.

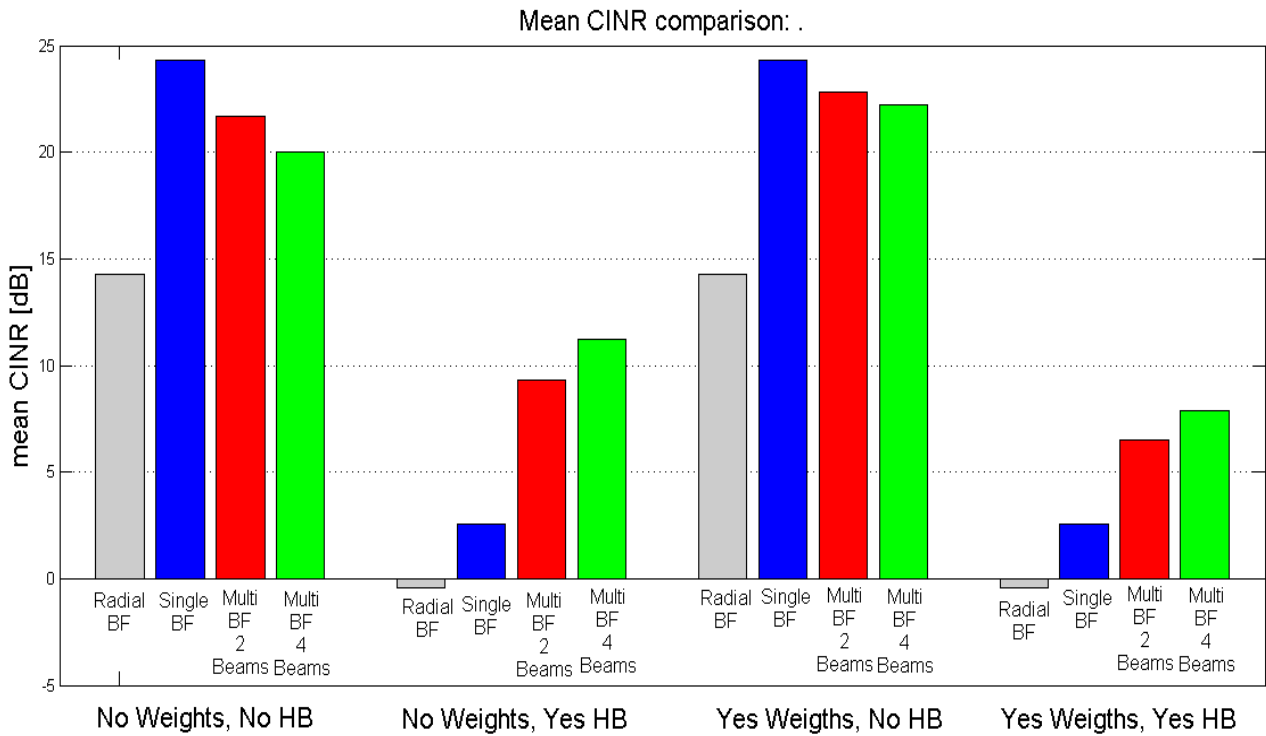


Fig.50: 24 RX average of mean CINR values for all cases.

Comparing now different Beams Order we achieve the results in Fig.51. What has been just said before, it is valid again: with HB having 4 beams leads successfully to a greater spatial diversity, whereas without HB having only 2 beams is better because is closer to the Single-beam BF case. Of course these outcomes strongly depend on our study case characteristics, on initial hypotheses, on unknown errors, on Ray Tracing model and so on, but they can be anyway generalized in order to get a whole picture of Beamforming techniques at mm-waves.

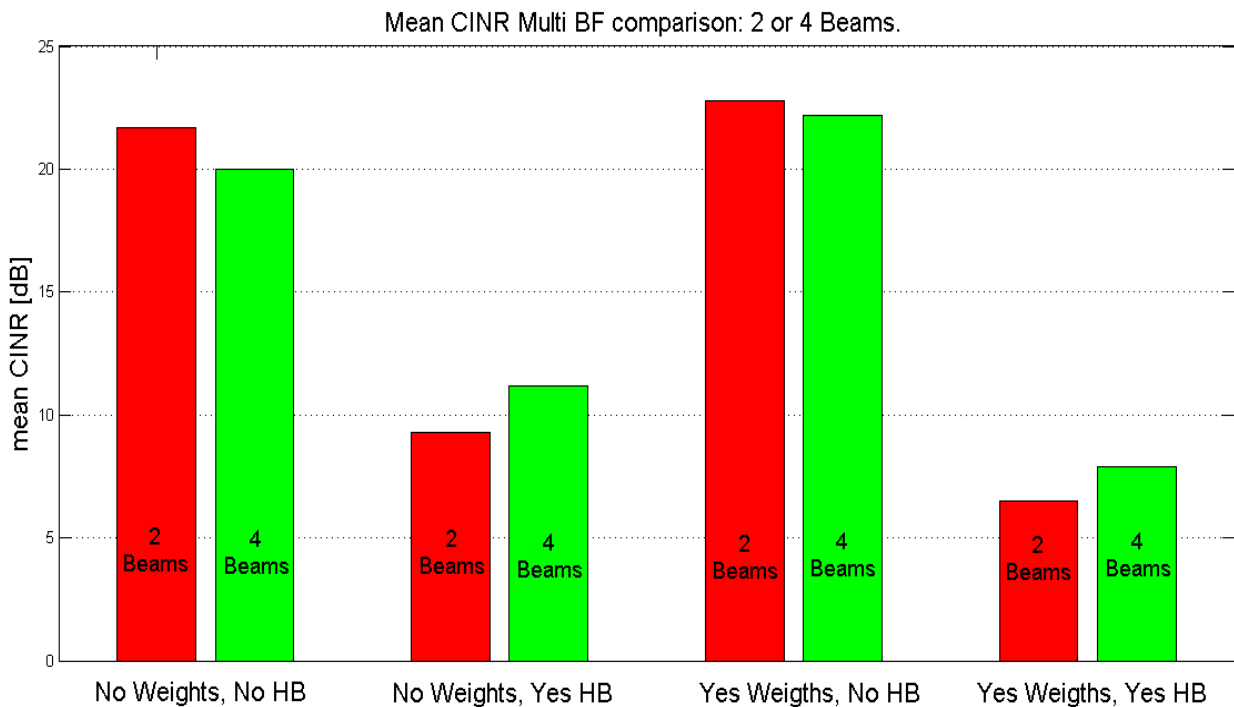


Fig.51: Multi-beams BF with BO = 2 and with BO = 4 comparison.

In the following section, in conclusion, we list all the CDFs function for the several cases -with and without weights and with BO=2 or BO=4- in order to remark statistically the deep change due to Human Blockage. The first big effect is the overall shifting to the left of the curves because the 30 dB power drop reduces simply the mean of all the C/Is values. But secondly we can not avoid to note that red and green lines, related to Multi-beams BF, are able to go further the blu line of Single-beam BF, thanks to spatial diversity, as already stated, (Fig.52-55).

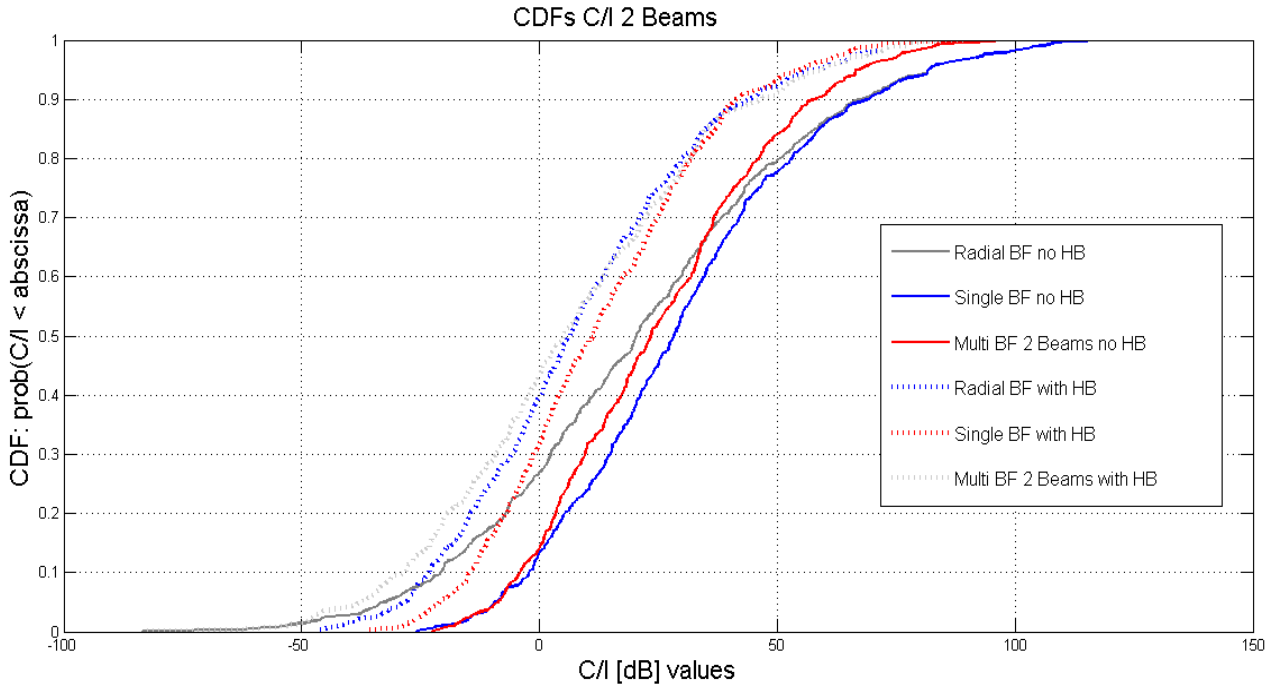


Fig.52: 2 beams with no weighting CDFs.

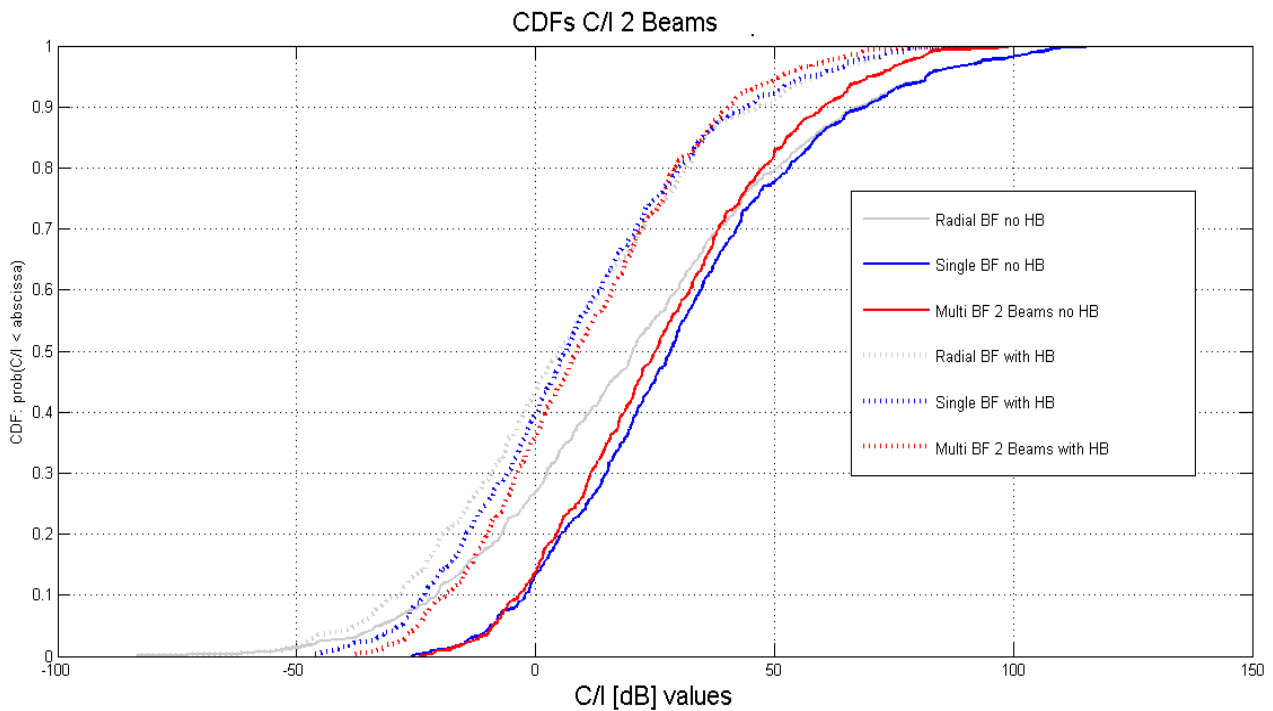


Fig.53: 2 beams with weighting CDFs.

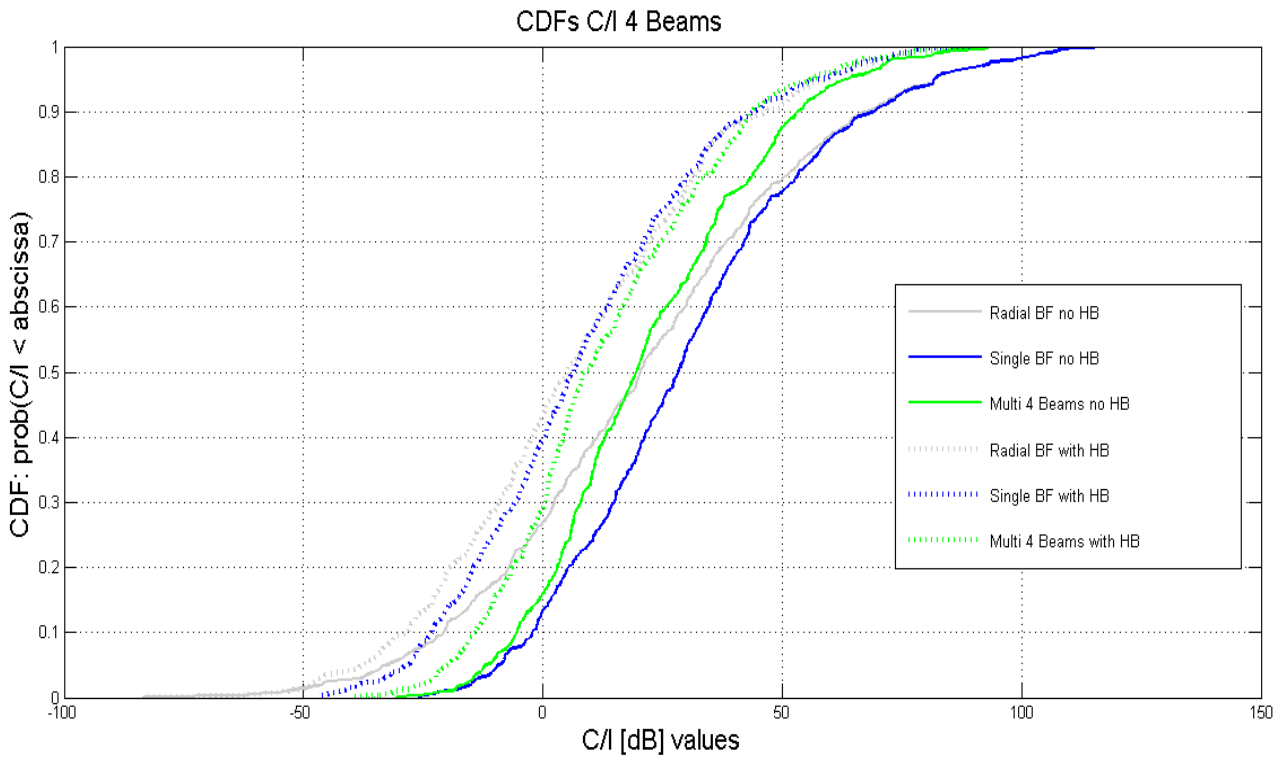


Fig.54: 4 beams with no weighting CDFs.

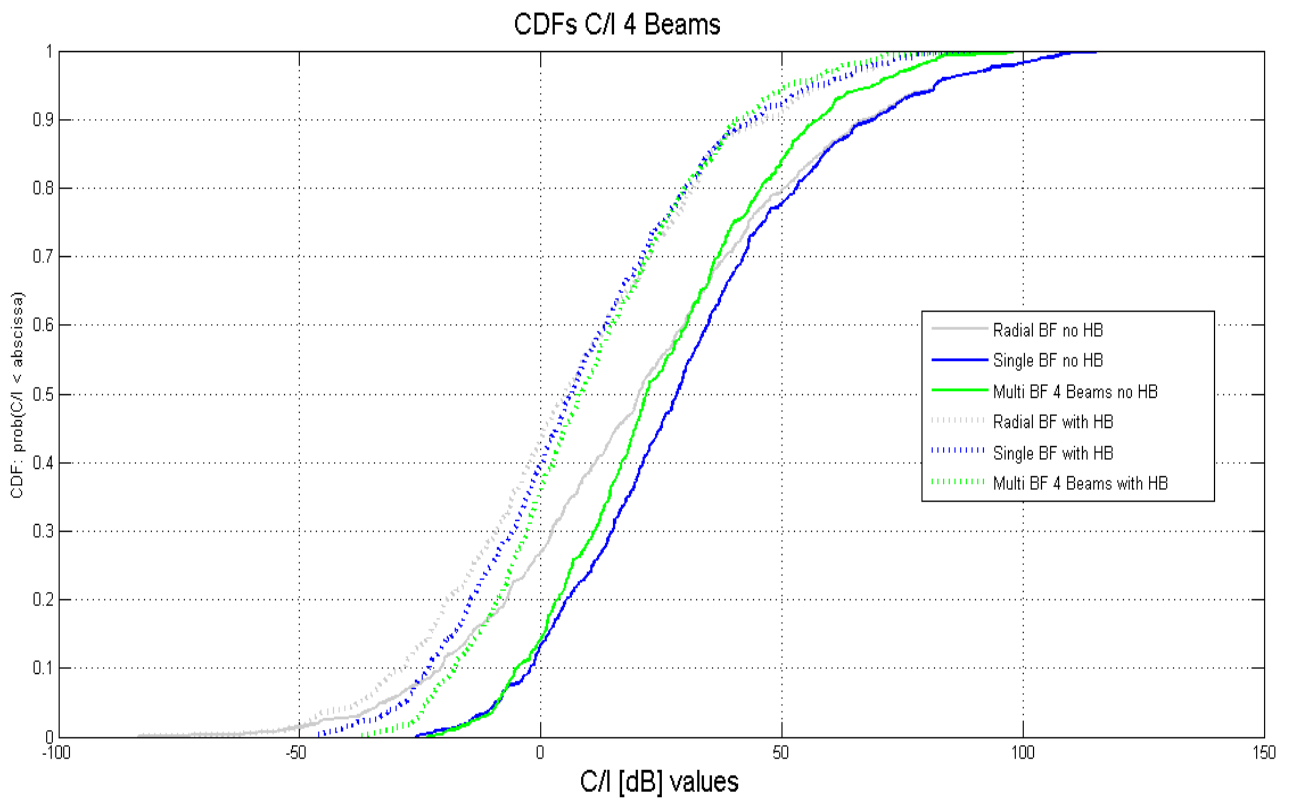


Fig.55: 4 beams with weighting CDFs.

## *Conclusions*

- 1) Despite for the entire comprehension of the mm-wave electromagnetism some essential radio channel investigations like measurements or propagation characterization are still to be completed for these kind of high frequencies communications, Beamforming will play a key role in future mm-wave systems to enable both spatial multiplexing and to cope with propagation impairments as confirmed by the simple study case simulation results.
- 2) Different Beamforming strategies have been checked on the basis of a RT approach: Single-beam BF case does its best in static conditions but could degrade significantly in presence of sudden, dynamic channel changes -in particular time-variant additional losses due to HB-. Multi-beams BF solution on the contrary has generally poorer performance in static conditions, but it allows a better robustness in dynamic conditions due to some diversity gain. A trade-off can be assumed to be the weighted Mutli-beams BF. As described in the Beamforming part, we are aware of the many issues that would pop up in phase of concrete design or implementation of such complex digital architectures -just think about the cost of such redundant circuits for example-.
- 3) Furthermore the promising Ray Tracing in real-time -embedded prediction- able to pilot totally or partially the BF, is a prospective that deserves further investigation but: it is valid to manage the HB issue with adaptive pattern configuration, it could be faster than standard “trial and error” codebook-based Beam Searching protocols and finally it does not need expensive changes moving from Single to Multi beams BF schemes choosing dynamically more then one best path.
- 4) Obviously the story does not end here: Diffuse Scattering effects, antenna polarization, multi-antenna systems at RXs, more realistic scenario description, more accurate 60Ghz tuned versions of RT, fully dynamic Human Blockage simulations, Physical layer signals integration, other interference combinations and so on are all missing parts that need to be taken into account in order to be free to say that the mm-wave “puzzle” is almost done.

## ***Bibliography:***

- [1] – Cisco White paper 2014, “Visual Networking Index: Forecast and Methodology, 2013–2018”.
- [2] – Cisco White paper 2014, “The Zettabyte Era: Trends and Analysis”.
- [3] – Ericsson “Mobility Report”, 2014.
- [4] – J.L Beylat, Bell Labs, Alcatel Lucent “5G: The Software Network and Virtualization Opportunities”, presentation hold at EuCNC, 2014.
- [5] – H. Moiin, Nokia “Looking ahead to 5G”, presentation hold at EuCNC. 2014.
- [6] – Wonil Roh, Samsung: “5G Mobile Communications for 2020 and beyond”, presentation hold at EuCNC. 2014.
- [7] – Wen Tong, Huawei: “5G goes beyond Smartphones”, presentation hold at EuCNC. 2014.
- [8] – Hansen, C.J., “WiGiG: Multi-gigabit wireless communications in the 60 GHz band”, IEEE Wireless Communications, 2011.
- [9] – Rappaport, T.S., S. Sun, R. Myzus, H. Zhao, Y. Azar, K. Wang, G.N. Wong, J.K. Schulz, M. Samimi, and F. Gutierrez, “Millimeter Wave Mobile Communication for 5G Cellular: It Will Work!”, IEEE Access, 2013.
- [10] – IEEE 802.15.3 amendment 2, 2009.
- [11] – ECMA 387 standard, 2010.
- [12] – IEEE 802.11ad amendment 3, 2012.
- [13] – WiGig White paper “WiGig and the future of seamless connectivity”, 2013.
- [14] – Wonil Roh, Ji-Yun Seol, JeongHo Park, Byunghwan Lee, Jaekon Lee, Yungsoo Kim, Jaeweon Cho, and Kyungwhoon Cheun, Farshid Aryanfar, “Millimeter-Wave Beamforming as an Enabling Technology for 5G Cellular Communications: Theoretical Feasibility and Prototype Results”, IEEE Communications Magazine, 2014.
- [15] – M.Coldrey, J.e. Berg, L.Manholm, C.Larsson, J. Hansryd, “Non-Line-of-Sight Small Cell Backhauling Using Microwave Technology”, IEEE Communication magazine, 2013.
- [16] – Tensorcom TC2522-Y 802.11ad SiP datasheet, 2014.
- [17] – Wilocity Wil6200 chipset datasheet, 2014
- [18] – Lei Wang, Yong-Xin Guo, Wei-Xing Sheng, “Wideband High-Gain 60-GHz LTCC L-Probe Patch Antenna Array With a Soft Surface”, IEEE Transactions on Antennas and Propagation, 2013.
- [19] – Takayuki Tsukizawa, Naganori Shirakata, Tadashi Morita, Koichiro Tanaka et al., “A Fully Integrated 60GHz CMOS Transceiver Chipset Based on WiGig/IEEE802.11ad with Built-In Self Calibration for Mobile Applications”, ISSCC, 2013.
- [20] – Mingjian Li, and Kwai-Man Luk, “Low-Cost Wideband Microstrip Antenna Array for 60-GHz Applications”, IEEE Transactions on Antennas and Propagation, 2014.
- [21] – Bing Zhang, Diane Titz,, Fabien Ferrero, Cyril Luxey, and Yue Ping Zhang “Integration of Quadruple Linearly-Polarized Microstrip Grid Array Antennas for 60-GHz Antenna-in-Package Applications”, IEEE transactions on components, packaging and manufacturing technology, 2013.
- [22] – V.Rizzoli, D.Masotti, “Sistemi d'antenna”.
- [23] – H. Van Trees, “Optimum Array Processing”, Wiley, 2002.
- [24] – Kraus, “Antennas”, Mc-Grawhill, 1988.
- [25] – Balanis, “Antenna Theory”, Wiley, 1982.
- [26] – Elliot, “Antenna Theory and Design”, Prentice Hall, 1981.
- [27] – Johnson, “Antenna Engineer Book”, Mc-Grawhill, 1993.
- [28] – Milligan, “Modern Antenna Design”, Mc-Grawhill, 1985.
- [29] – Stutzman and Tiele, “Antenna Theory and Design”, Wiley, 1981.
- [30] – Skolnik, “Radar Handbook”, Mc-Grawhill, 1990.
- [31] – Liang Zhou and Yoji Ohashi, “Efficient Codebook-Based MIMO Beamforming for Millimeter-Wave WLANs”, IEEE PIMRC, 2012.
- [32] – Junyi Wang, Zhou Lan, Chang-Woo Pyo, Tuncer Baykas, Chin-Sean Sum, M Azizur Rahman, Jing Gao, Ryuhei Funada, Fumihide Kojima, Hiroshi Harada and Shuzo Kato “A Pro-Active Beamforming Protocol for Multi-Gbps Millimeter-Wave WPAN Systems”, IEEE WCNC, 2010.
- [33] – Wei Feng, Zhenyu Xiao, Depeng Jin, and Lieguang Zeng “Circular-Antenna-Array-Based Codebook Design and Training Method for 60GHz Beamforming”, IEEE WCNC, 2013.
- [34] – Li Chen, Ying Yang, Xiaohui Chen, Weidong Wang “Multi-stage beamforming codebook for 60GHz WPAN”, CHINACOM, 2011.

- [35] – Bile Peng, Sebastian Priebe, Thomas Kürner “Fast Beam Searching Concept for Indoor Terahertz Communications”, EuCAP, 2014.
- [36] – Xiaoyi Zhu, Angela Doufexi, and Taskin Kocak, “Beamforming Performance Analysis for OFDM Based IEEE 802.11ad Millimeter-Wave WPANs”, IEEE, 2011.
- [37] – Changming Zhang, Zhenyu Xiao, Hao Wu, Lieguang Zeng and Depeng Jin “Performance Analysis on the OFDM PHY of IEEE 802.11ad Standard”, ICCP, 2011.
- [38] – O. Bazan “A Survey On MAC Protocols for Wireless Adhoc Networks with Beamforming Antennas”, IEEE Communications Surveys & Tutorials, 2012.
- [39] – Degli-Esposti, V., D. Guiducci, A. de’ Marsi, P. Azzi, and F. Fuschini “An advanced field prediction model including diffuse scattering”, IEEE Trans. Antennas Propagation, 2004.
- [40] – Degli-Esposti, V., F. Fuschini, E.M. Vitucci, and G. Falciasecca “Measurement and Modelling of Scattering From Buildings”, IEEE Trans. Antennas Propagation, 2007.
- [41] – Degli-Esposti, V., F. Fuschini, and E. M. Vitucci “A fast model for distributed scattering from buildings, EuCAP, 2009.
- [42] – Vitucci, E.M, F. Mani, V. Degli-Esposti, C. Oestges “Polarimetric Properties of Diffuse Scattering from Building Walls: Experimental Parameterization of a Ray-Tracing Model”, IEEE Trans. Antennas Propagation, 2012.
- [43] – Mani, F., E. M. Vitucci, F. Quitin, V. Degli-Esposti, C. Oestges “Parameterization of a Polarimetric Diffuse Scattering Model in Indoor Environments”, IEEE Trans. Antennas Propagation, 2014.
- [44] – Jacob, M., S. Priebe, T. Kurner, M. Peter, M. Wisotzki, R. Felbecker, and W. Keusgen “Extension and validation of the IEEE 802.11ad 60 GHz human blockage model”, EuCAP, 2013.;
- [45] – Peter, W., W. Keusgen, and R. Felbecker, “Measurement and ray-tracing simulation of the 60 GHz indoor broadband channel: model accuracy and parameterization”, EuCAP, 2007.
- [46] – Priebe, S., M. Kannicht, M. Jacob, and T. Kürner , “Ultra Broadband Indoor Channel Measurements and Calibrated Ray Tracing Propagation Modeling at THz Frequencies”, Journal of Communications and Networks, 2013.
- [47] – Larew, S.G., T.A. Thomas, M. Cudak, and A. Ghosh “Air Interface and Ray Tracing Study for 5G Millimeter Wave Communications”, IEEE Globecom Workshops, 2013.
- [48] – D. Dupleich, F. Fuschini, R. Mueller, E. Vitucci, C. Schneider, V. Degli Esposti and R. Thöma “Directional characterization of the 60 GHz indoor-office channel” 2014.
- [49] – Lu, J., D. Steinbach, P. Cabrol, P. Pietraski, and R.V. Pragada, “Propagation Characterization of an Office Building in the 60 GHz Band”, EuCAP, 2014.
- [50] – Cuinas, I, J.P. Pugliese, A. Hammoudeh, and M.G. Sanchez , “Frequency dependence of dielectric constant of construction materials in microwave and millimeter-wave bands”, Microwave and Optical Technology Letters, 2001.
- [51] – V. Degli Esposti, E. Tarantino, M. Barbiroli, F. Fuschini and G. Riva “Embedded ray tracing techniques to improve performance in MIMO mobile radio systems : a preliminary study”, IEEE 2011.
- [52] – ETSI, “Broadband Radio Access Networks (BRAN); 60 GHz Multiple-Gigabit WAS/RLAN Systems”, 2009.
- [53] – CEPT, “ERC Recommendation 70-03; Relating to the Use of Short Range Devices (SRD) ”, 2014.
- [54] – Martin Jacob, Sebastian Priebe, Alexander Maltsev, Artyom Lomayev, Vinko Erceg, Thomas Kürner, “A Ray Tracing Based Stochastic Human Blockage Model for the IEEE 802.11ad 60 GHz Channel Model”, 2011.
- [55] – Martin Jacob, Sebastian Priebe and Thomas Kurner, Michael Peter, Mike Wisotzki, Robert Felbecker and Wilhelm Keusgen, “Fundamental Analyses of 60 GHz Human Blockage”, 2013.